

Zeitschrift: IABSE reports = Rapports AIPC = IVBH Berichte
Band: 45 (1983)

Rubrik: Session 3: Mathematical and physical models

Nutzungsbedingungen

Die ETH-Bibliothek ist die Anbieterin der digitalisierten Zeitschriften auf E-Periodica. Sie besitzt keine Urheberrechte an den Zeitschriften und ist nicht verantwortlich für deren Inhalte. Die Rechte liegen in der Regel bei den Herausgebern beziehungsweise den externen Rechteinhabern. Das Veröffentlichen von Bildern in Print- und Online-Publikationen sowie auf Social Media-Kanälen oder Webseiten ist nur mit vorheriger Genehmigung der Rechteinhaber erlaubt. [Mehr erfahren](#)

Conditions d'utilisation

L'ETH Library est le fournisseur des revues numérisées. Elle ne détient aucun droit d'auteur sur les revues et n'est pas responsable de leur contenu. En règle générale, les droits sont détenus par les éditeurs ou les détenteurs de droits externes. La reproduction d'images dans des publications imprimées ou en ligne ainsi que sur des canaux de médias sociaux ou des sites web n'est autorisée qu'avec l'accord préalable des détenteurs des droits. [En savoir plus](#)

Terms of use

The ETH Library is the provider of the digitised journals. It does not own any copyrights to the journals and is not responsible for their content. The rights usually lie with the publishers or the external rights holders. Publishing images in print and online publications, as well as on social media channels or websites, is only permitted with the prior consent of the rights holders. [Find out more](#)

Download PDF: 05.09.2025

ETH-Bibliothek Zürich, E-Periodica, <https://www.e-periodica.ch>



SESSION 3

Mathematical and Physical Models

Modèles mathématiques et physiques

Mathematische und physikalische Modelle

Leere Seite
Blank page
Page vide

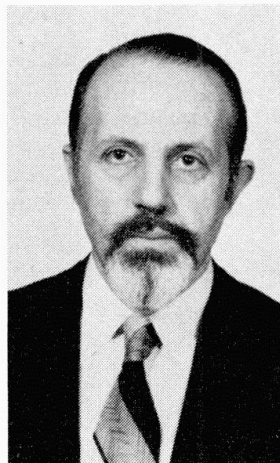
Physical and Mathematical Models for Re-design of Damaged Structures

Modèles pour l'évaluation de structures endommagées

Berechnungsmodelle zur Verstärkung von Bauwerken

T.P. TASSIOS

Professor
Nat. Tech. University
Athens, Greece



T.P. Tassios, full Professor of reinforced concrete structures at the N.T.U., Athens, is the author of 120 papers and research reports on theory of elasticity, concrete technology, seismic behaviour of R.C., etc, in several languages. Prof. Tassios is member of the Administrative Council of CEB and chairman of some international committees.

SUMMARY

This report is an introduction to the computational methods regarding assessment of damaged buildings, redimensioning of repaired and/or strengthened elements, as well as redistribution of action-effects after intervention. Several physical and analytical models are presented. Revised partial safety factors for such a redesign are also discussed.

RESUME

Le présent rapport est une introduction aux méthodes de calcul concernant l'évaluation des constructions endommagées, le dimensionnement des éléments réparés ou renforcés, ainsi que la redistribution de sollicitation après l'intervention. Plusieurs modèles physiques et analytiques sont présentés. De nouveaux coefficients de sécurité partiels sont discutés.

ZUSAMMENFASSUNG

Dieser Bericht dient als Einführung in die Berechnungsmethoden hinsichtlich der Beurteilung von beschädigten Bauwerken, der Neubemessung von ausgebesserten und/oder verstärkten Elementen sowie der Neuverteilung der Beanspruchungen nach dem Eingriff. Verschiedene physikalische und analytische Modelle werden aufgezeigt. Neue Teilsicherheitsfaktoren werden diskutiert.



INTRODUCTION

a) A check-list of steps

Fig. 1 is an attempt to summarise the possible consecutive steps usually taken after the damage of a structure or after the problem of its strengthening is arisen.

In this connection, a glossary should also be reminded very briefly:

Assessment = Evaluation of bearing capacity

Intervention = Repair and/or strengthening ("R+S")

Repair = Reinstatement of the initial mechanical characteristics

Strengthening = Instating of characteristics higher than the initial ones.

Redesign = Design procedures concerning interventions.

b) Modeling

In Redesign, several new situations are faced (s. §c here below); rather unclear structural conditions call for complicated computational methods. Therefore, in Redesign much more than in Design of new structures, m o d e l i n g is needed: A possibly clear, reasonably simplified representation of a system serves for an approximate prediction of its behaviour. A summary of the terminology regarding models in engineering is shown in Fig. 2.

c) A note on the contents

Redesign and Strengthening (R+S) has to do with several i n t e r f a c e s, which are due to the damage itself or are created by the intervention: n e w materials are added to the existing (damaged or weak) building elements, e.g. concrete to concrete, epoxy resin to concrete, steel to concrete (acting transversally or axially), steel to steel acting through a welded seam, etc. Consequently, load transfer from the existing (damaged or weak) element to the additional "reinforcing" materials is carried-out through discontinuities, by means of u n c o n v e n t i o n a l mechanisms like friction, dowel action, large pull-out actions, etc. The systematic study of these mechanisms (a kind of a new Strength of Materials for the n o n - c o n t i n u u m) seems to be a fundamental prerequisite for the design of repaired and/or strengthened structures. That is why Part I of this Report is devoted to a very brief presentation of such topics. Part II goes from "cross-sections" to "building elements"; the knowledge of the aforementioned load transfer mechanisms is used for the assessment of residual capacity of damaged elements, as well as for their re-dimensioning after intervention.

Sometimes new action-effects have to be taken into account for such an assessment or redimensioning; and this is the scope of Part III, which refers to the level of the whole s t r u c t u r e s and the r e d i s t r i b u t i o n of action-effects taking place at this level.

The presentation of the redesign process is completed by a short Part IV on the r e l i a b i l i t y or repair and/or strengthening interventions: revised partial safety factors are introduced, to cover additional uncertainties related to R+S technologies or models.

d) Comments

The arrangement of the contents of this Report is mainly dictated by mechanical terms (type of action, type of structural member) rather than by R+S techniques or materials; it may be said that such a presentation is not in favour of the practicability of this document. On the other hand, it has to be admitted that well established and tested models in this area are rather scarce, whereas some of them need to be c a l i b r a t e d (by experiment or by means of trial calculations).

Last but not least, this Report should be extremely short (in comparison to what it would be needed for such a practical topic).

For all these three reasons, this Report can not be considered as a compendium of models to be directly applied in the analysis and dimensioning of damaged or weak structures, but rather as a s t i m u l u s for further r a t i o n a l i s a t i o n of this process, and as an i n v i t a t i o n for substantial papers, filling the existing gaps of knowledge.

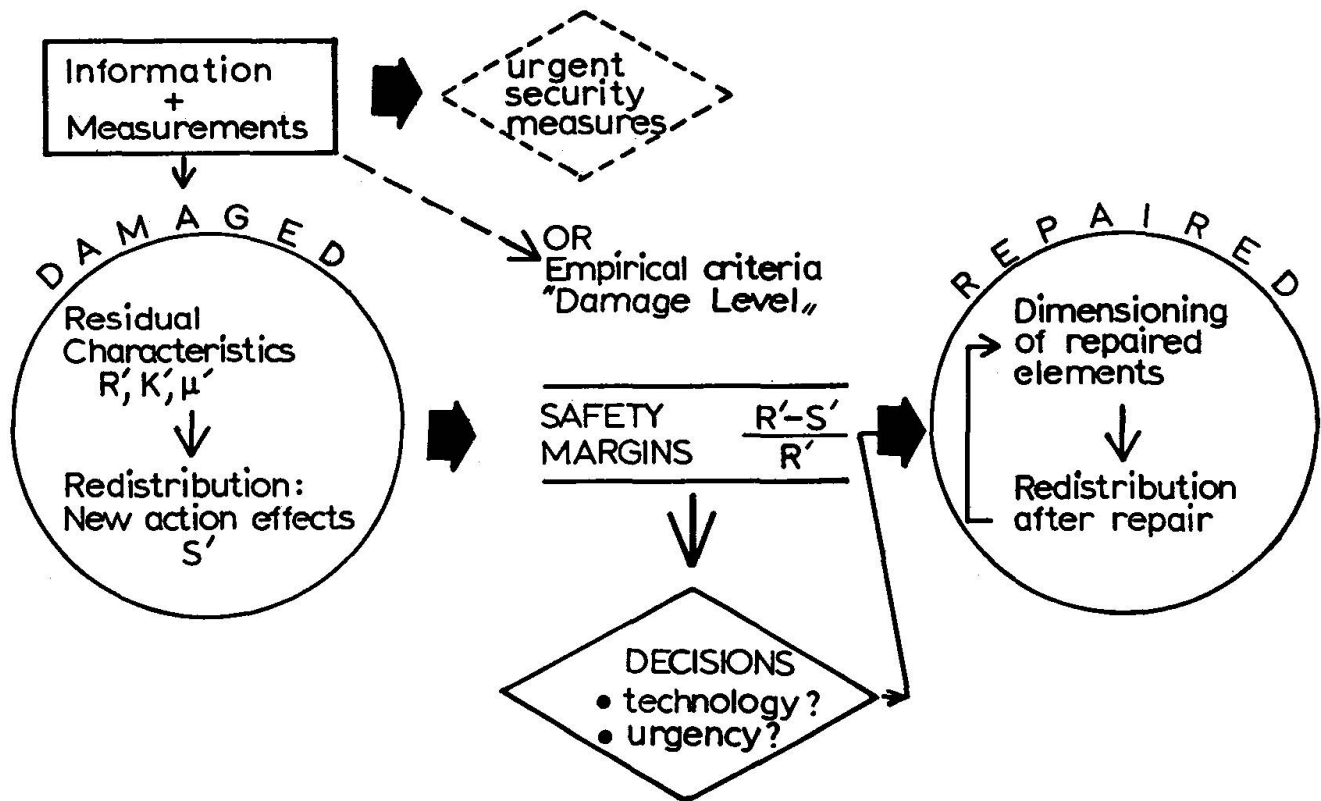


Fig. 1: A thinking model for redesign of buildings. R = strength, S = action-effect, K = stiffness, μ = ductility

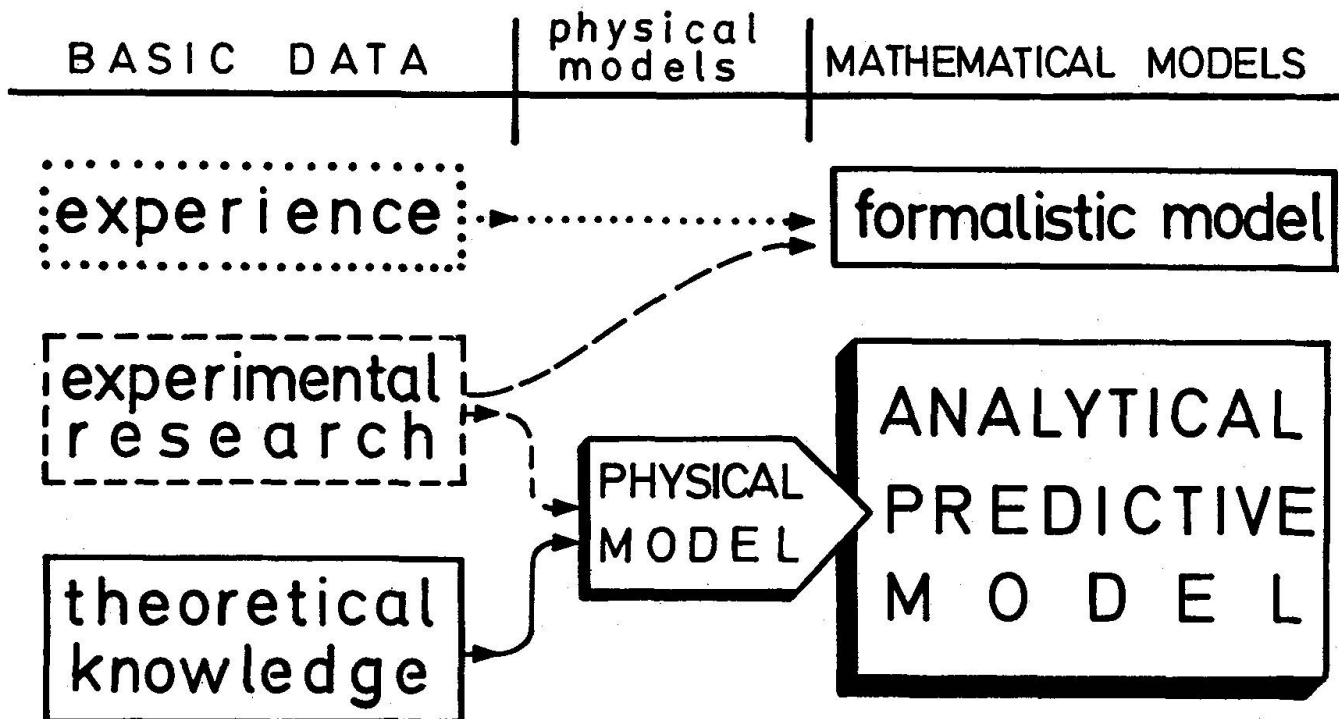


Fig. 2: A formalistic model is based on empirical data only and not on a physical model (i.e. on a rational knowledge about the structure and the function of the system described)



Part I: Load Transfer Mechanisms through Interfaces and
Corresponding Constitutive Laws

1. BY MEANS OF NON-METALLIC MATERIALS

1.1. Compression

Through **precracked** surfaces of concrete, TASSIOS and PLAÏNÈS, 1981, have proposed the model shown in Fig. 3: During reloading after tensional cracking, compressive forces are undertaken by the concrete, before full recovering of tensional deformation: The protruding elements constituting the rough interface of a crack are taking a much earlier contact, due to their transversal micro-displacements. Dust grains entrapped in the crack may also contribute to such an early contact. On Fig. 3a, only overall deformations (not strains) are presented, since a large part of the total deformation is highly localised very near to the cracks where local slips and crushings are observed.

Through **technically made interfaces**, compression is producing additional deformations due to the imperfections of compaction and lateral confinement near the interface. Thus, normal or polymer modified concrete near the interface, within a limited length " l_0 ", may exhibit moduli of elasticity " E_0 " lower than their full mass modulus " E ". Consequently, $\Delta l = \frac{\sigma}{E} \cdot l \cdot (1 + \frac{l_0}{E_0 \cdot E})$, the correction factor depending on the compaction pressure and the fluidity of the additional material. On the other hand, additional compressive deformation due to pressure injected cracks may be easily estimated if crack's width, modulus of elasticity and creep coefficient of filling material are known. In this connection, the following numerical data may be used for epoxy resins when specific measurements are not available:

$$E_{\text{resin}} = 3500 \text{ MPa} (1000 \div 30000), \quad \phi_{\text{resin}} \approx 3.$$

1.2. Tension and adhesion

Terminology is reminded on Fig. 4. Reference is made here only to adhesion; two constitutive curves are reproduced on Fig. 5 connecting **local** adhesion stress to **local** slip. An **extremely large** sensitivity of these curves is expected versus surface treatment, curing, materials' composition, etc (see, i.a., BATE, 1957, DASCHNER, 1976), and STEINWEDE, 1977).

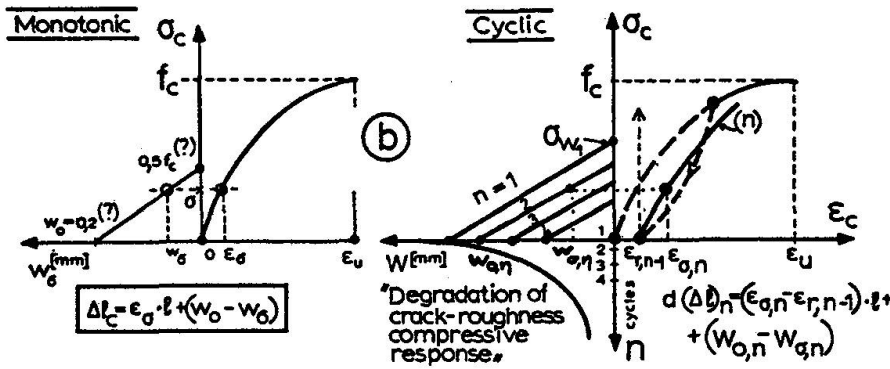
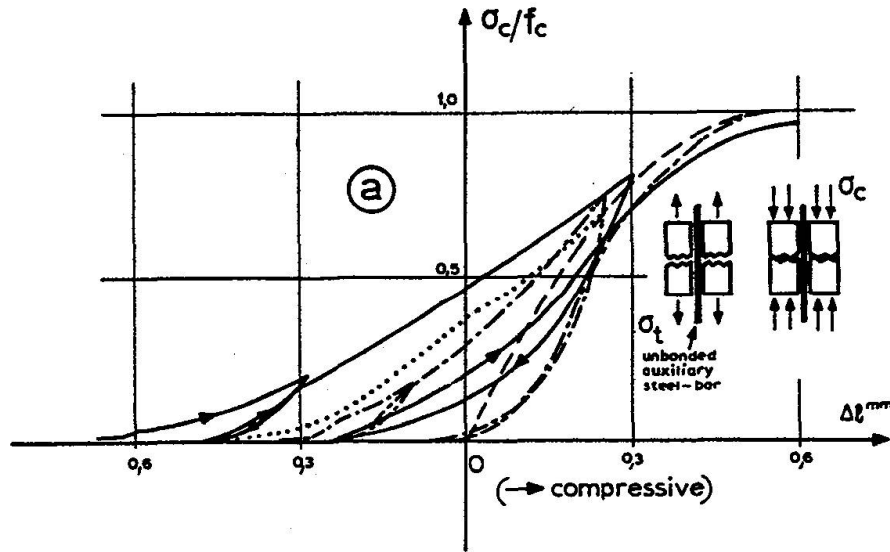


Fig. 3: Cyclic compression of pre-cracked concrete

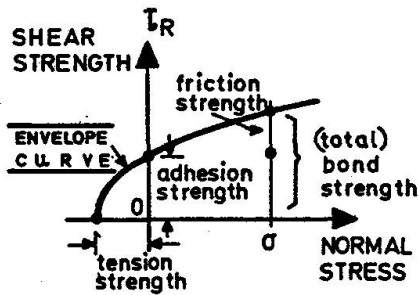


Fig. 4: Terminology regarding tension and shear strength

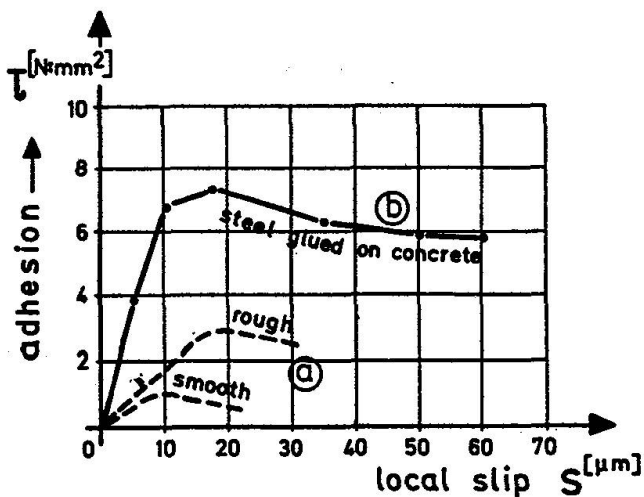


Fig. 5: Constitutive curves of adhesion (local stress-local slip)
a) Concrete to concrete through bonding agent, (Hanson, 1960)
b) Steel sheet glued to concrete by means of epoxy resin, (based on Ladner et al., 1981)



1.3. Friction

It has first to be reminded that friction sources are usually distinguished into "micro-roughness" (second order asperities) and "macro-roughness" (finite geometrical anomalies along the interface); aggregates' interlocking may be classified into this second category. This chapter is dealing only with friction due to micro-roughness; macro-roughness is considered in §4.1 of this Part of the Report.

As **every** other mechanical resistance, friction needs deformation (slippage in this cases) in order to be mobilised. Therefore, full knowledge of this mechanism of load transfer is acquainted only through a constitutive law connecting friction-shear stress " τ_f " and corresponding slip " s ".

Under **monotonic** loading, concrete-to-concrete friction may be modeled as shown in Fig. 6, based on experimental data of TASSIOS and VASSILIOU, 1975, as well as TASSIOS and VINTZÉLEOU, 1978.

For masonry, Fig. 7 shows only friction coefficients as a function of the average normal pressure acting locally on the cracked section. Under **cyclic** loading, concrete-to-concrete friction mobilised may be roughly estimated by means of the formalistic model shown in Fig. 8, derived from experimental data of F. ELEIOTT, 1974, initial point "1" (τ_0, s_1) is supposed to be known on the basis of the models valid for monotonic loading.

2. BY MEANS OF STEEL

2.1. Dowel actions

2.1.1. Quasi_elastic_stage: There is a classical modeling of the transversal action of steel bars imbedded in concrete ("dowel action") under monotonic loading, based on the subgrade reaction hypothesis (Winkler space), as commonly used for the estimation of the behaviour of piles under horizontal loading (Fig.9.a):

$$D \cong \frac{1}{2} \frac{K_c d_b}{\lambda} s, \quad \lambda = \sqrt[4]{\frac{K_c d_b}{4E_s J_s}}, \quad (\text{M. Hetényi, 1946}),$$

$K_c \cong E_c : 1,5 d_b$ (s. Timoshenko, 1934). Several simplifications may lead to the expressions shown in Fig. 10, taking also into account data from §2.1.2.

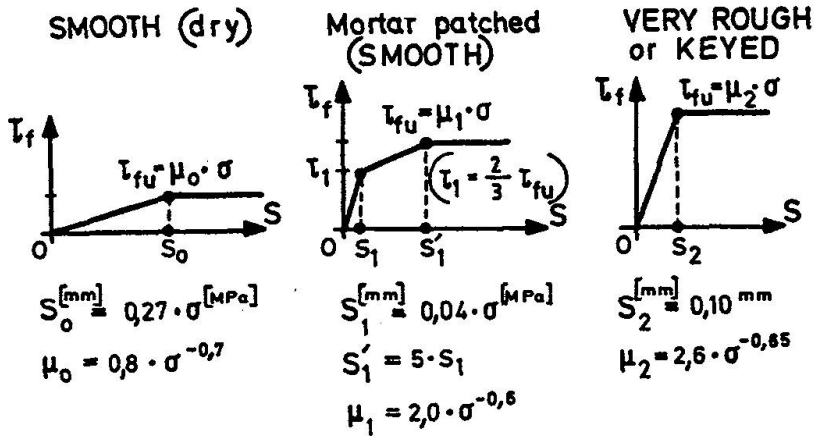


Fig. 6: Formalistic models for concrete-to-concrete friction, as a function of normal compressive stress " σ " (MPa) and relative displacement " s " (mm)

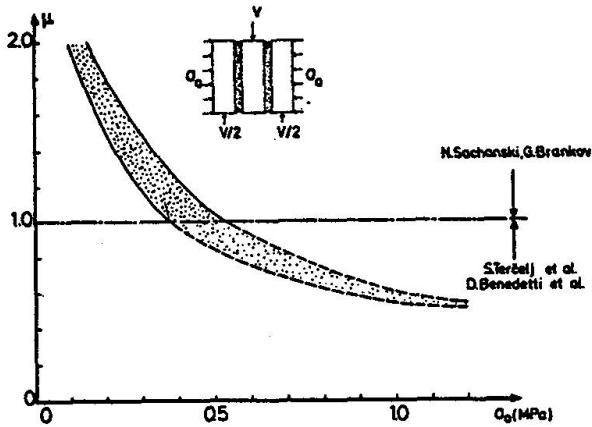


Fig. 7: Friction coefficients for masonry as a function of the average normal stress.

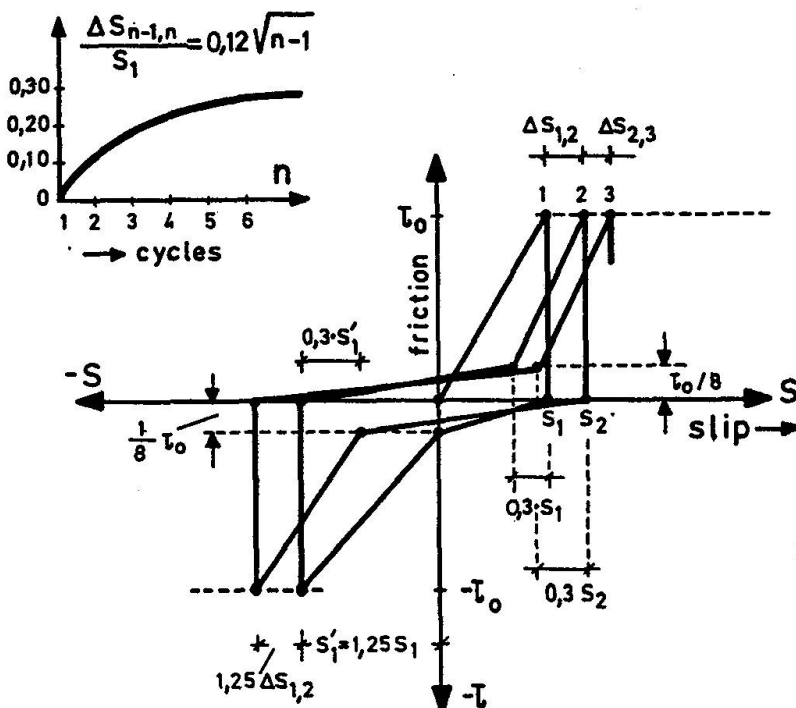


Fig. 8: A formalistic model for concrete-to-concrete friction under cyclic loading (based on Eleiott, 1974)



2.1.2. Plastic compressive stage

Here again, for the estimation of the ultimate capacity of a dowel embedded in **non-cracked** concrete (large concrete covers and/or appropriate confinement), the plastic soil-pile model may also be used.

The local strength of the concrete is reached and a plastic hinge is formed in the dowel at a small depth. Two mechanisms are contributing to a considerable increase of the local resistance f_{cc}^* of the concrete above the plastic hinge:

- Compression is applied to a very small length, resulting in a higher concrete strength behind this area,
- Longer rupture lines are developed across the dowel, offering a high ultimate resistance of concrete.

According to existing theoretical and experimental evidence (L. Reese, 1958, B. Broms, 1964, H. Matlock, 1970, H. Poulos, 1971, for piles in cohesive soils, and H. Dulacska, 1972, for dowels) the final local resistance f_{cc}^* is approximately equal to 4 to 6 times the unconfined strength f_{cc} .

Therefore (Fig. 9.b):

$$D_u \approx 0,85 f_{cc} \cdot d_b \cdot l_o, \quad l_o \approx \frac{D_u}{4 f_{cc} d_b}$$

$$M_u \approx D_u l_o - D_u \cdot 0,4 l_o \approx 0,6 D_u l_o$$

$$M_u \approx \frac{3}{2} \frac{\pi d_b^3}{32} \cdot f_{sy} \quad (\text{plastic yield moment})$$

$$\therefore D_u \approx d_b^2 \sqrt{f_{cc} \cdot f_{sy}}.$$

Of course, the above simple models may be corrected by direct experimental measurements of " D_u ". Thus, B. Rasmussen (1962) has found:

$$D_u \approx 1,3 \cdot d_b^2 \sqrt{f_{cc} \cdot f_{sy}}.$$

2.1.3. Post cracking stage: After longitudinal splitting, due to tensile stresses σ_{ct} (Fig. 11,i), the length l_{cr} of the bar is not fully supported (Fig. 11, ii); an equivalent length l_{eq} of a cantilever is sought, having the same additional deflection, so that :

$$S_{tot} = S_{cr} + \frac{D - D_{cr}}{3 E_s J_s} l_{eq}^3, \quad l_{eq} \approx \lambda \cdot \frac{D}{f_{ct} d_b}$$

(in this expression, deflection due the elastic angle of rotation at the end of the non-cracked length is neglected), where

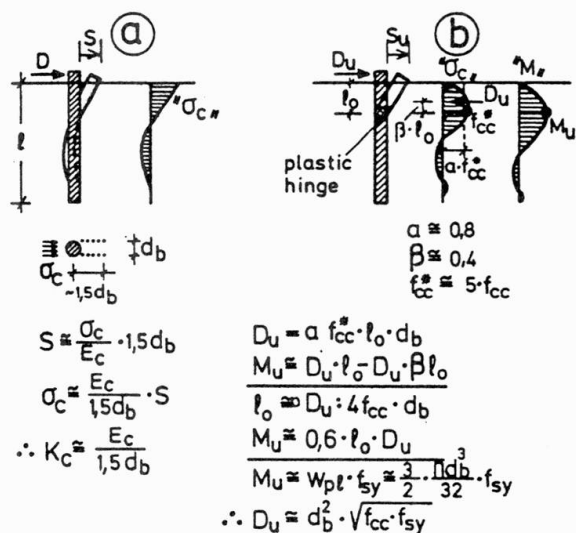


Fig. 9: Quasi-elastic (a) and plastic compressive (b) models for dowel action

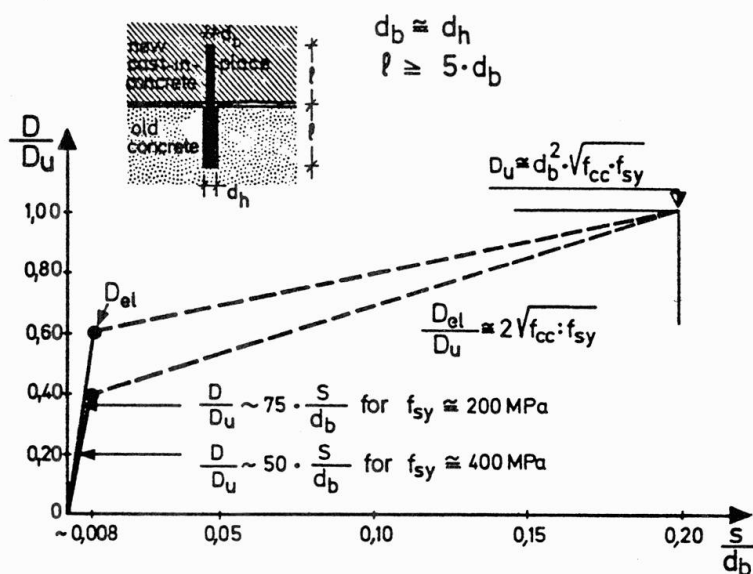


Fig. 10: Quasi-elastic and plastic compressive stage for dowels embedded in non-cracked concrete. The limit value $s_u:d_b = 0,2$ is based on data by J. Verdeyen and J. Gillet (1967) for piles in a cohesive soil

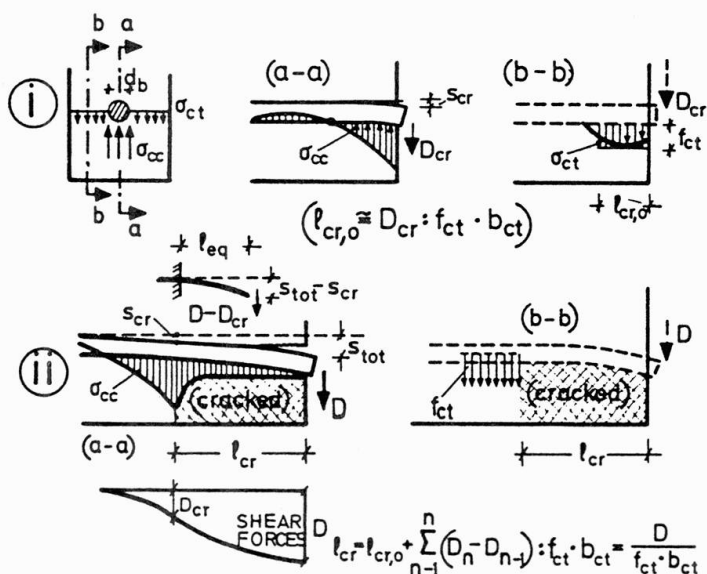


Fig. 11: A qualitative model for post-cracking displacement s_{tot} due to dowel action



s_{cr} = dowel displacement corresponding to the cracking load D_{cr} ; this displacement is calculated by means of an "elastic foundation" model (§2.1.1).

E_s, J_s = modulus of elasticity and inertia moment of the steel bar

$l_{eq} = \lambda \cdot l_{cr}$, equivalent unsupported length of the bar

λ = empirical factor (estimated around the value of 1/3 by VINTZÉLEOU, TASSIOS, 1982).

f_{ct} = tensile strength of concrete

b_{ct} = net width of the section

D_{cr} = cracking load, estimated

On the basis of the distribution of compressive quasi-elastic stresses along the dowel: effective length $\frac{\pi}{2} \cdot \frac{1}{\lambda}$, for equilibrium

$$D_{cr} = \frac{3}{4} b_{ct} \cdot \left(\frac{\pi}{2} \cdot \frac{1}{\lambda} \right) f_{ctm} \approx 1,9 \cdot b_{ct} \cdot d_b \cdot f_{ctm}, \quad \left(\lambda = \sqrt[4]{\frac{k_c d_b}{4 E_s J_s}} \right).$$

In what follows, this limit load has been empirically taken equal to $0,4 \cdot D_u$ (comp. Fig.10); for higher loads plastic phenomena appear. Thus, if the ultimate load D_u is also known (s. §2.1.2), the load/displacement relationship may be approximately represented by the expression

$$s_{tot} = s_{cr} + \left(\frac{f_{sy}}{215} \right) \left(\frac{f_{sy}}{f_c} \right) \left(\frac{d_b}{b_{ct}} \right)^3 \left[\left(\frac{D}{D_u} \right)^4 - 0,4 \left(\frac{D}{D_u} \right)^3 \right] \cdot d_b.$$

Here again, an oversimplification could be introduced: Since this expression is valid for $0,4 < D:D_u < 1,0$, an average value $D:D_u = 0,7$ could be used in the following transformed expression, together with mean values for $f_{sy}:f_c \approx 15$, $b_{ct}:d_b = 3,5$ and $f_{sy} = 420$, (neglecting the small value " s_{cr} "):

$$s = 1,95 \cdot 15 \cdot \frac{1}{43} \left(\frac{D}{D_u} \right)^4 \cdot \left(1 - 0,4 \cdot \frac{1}{0,7} \right) \cdot d_b \approx 0,3 d_b \left(\frac{D}{D_u} \right)^4,$$

$$\text{or, for } d_b \approx 12 \div 22^{mm}, \quad \frac{D}{D_u} \approx 0,7 \sqrt[4]{s^{mm}}.$$

This very rough approximation has also been found on the basis of experimental data presented in VINTZÉLEOU, TASSIOS, 1982, (s. also Fig.12).

Regarding cyclic loading, some formalistic data are shown in Fig.13, based on the experimental findings presented in VINTZÉLEOU, TASSIOS, 1982; their validity seems to be rather limited.

2.2. Bond actions

2.2.1. Local bond - local slip models

For a large category of phenomena of structural behaviour of rein-

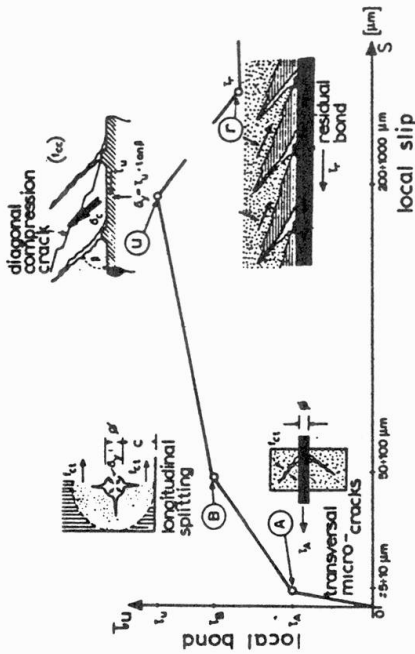


Fig. 14: A physical model explaining several characteristic situations of concrete surrounding a stressed steel bar. Simple predictive expressions are also given for the corresponding bond stress values in Tassios, 1979.

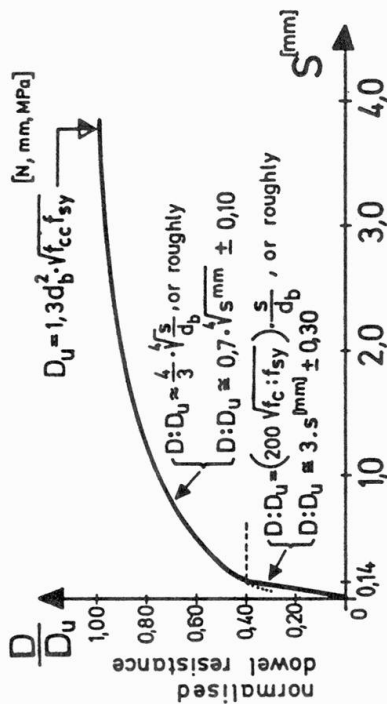


Fig. 12: An oversimplified constitutive law for dowel force-displacement, before and after splitting cracks have appeared

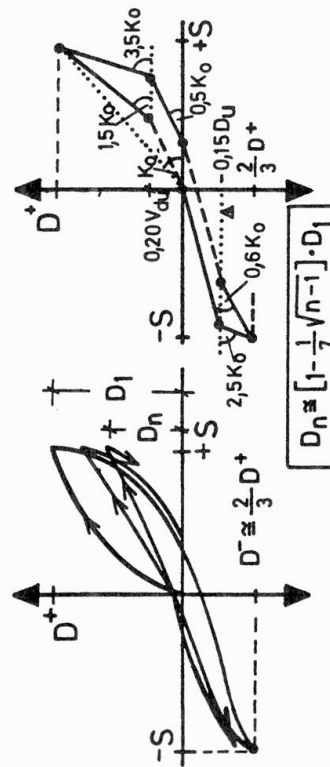


Fig. 13: A formalistic model for fully reversed (displacement controlled) dowel action

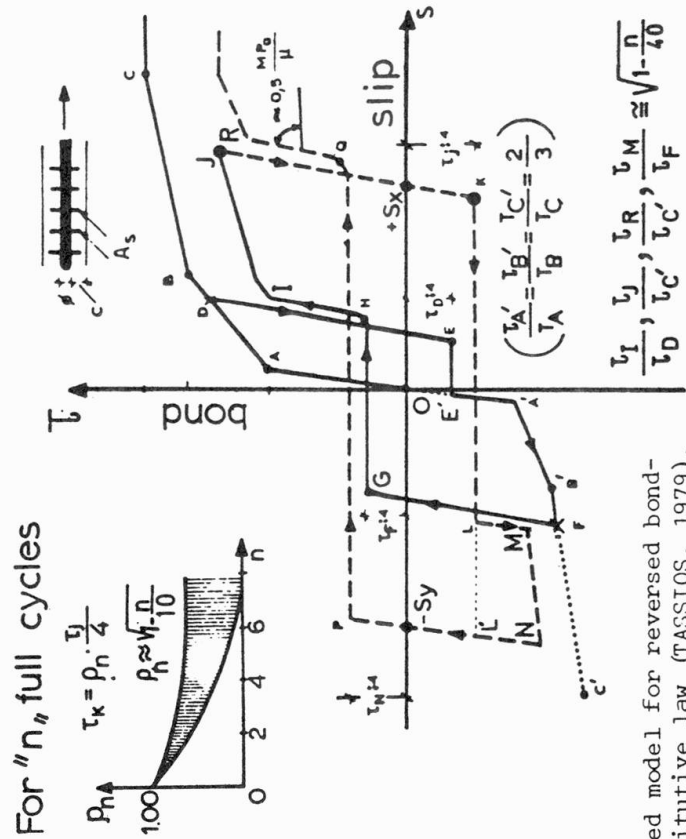


Fig. 15: A simplified model for reversed bond-slip constitutive law (TASSIOS, 1979).

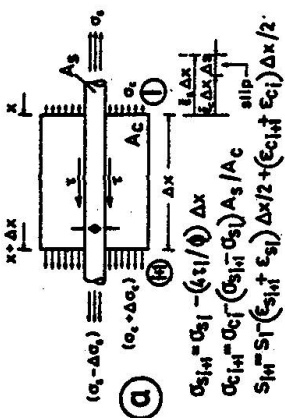


Fig. 19: a) Stresses and strains on a finite length of a R.C. element
b) Boundary conditions of a pull-out specimen of known effective concrete section.

Fig. 16: A detailed model for cyclic bond-slip actions (ELINGHOUSEN 1982).

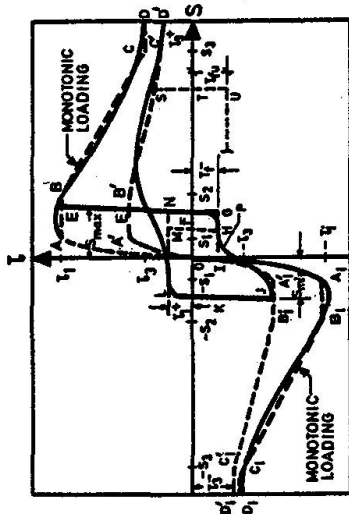


Fig. 20: Pull-out/push-in cyclic behaviour predicted by the local-bond local-slip approach (TASSIOS, PAPARIZOS, 1982)

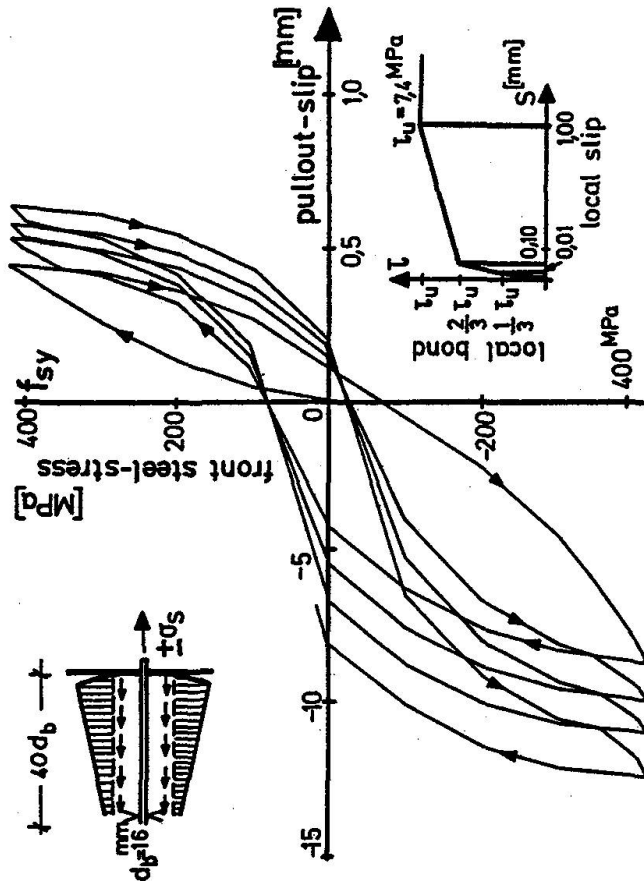


Fig. 17: Bond-slip-creep under bond stress " τ " may be estimated by means of the expression $\Delta s_{t,n} = \varphi_1 \cdot \varphi_n \cdot s_1$

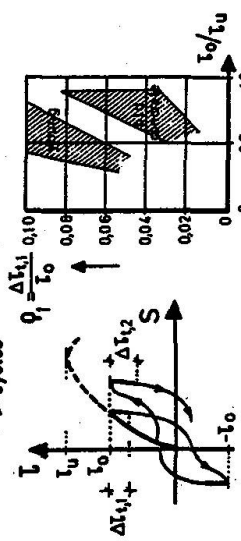
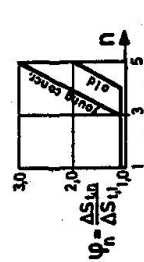
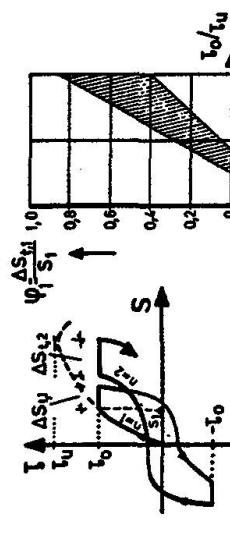
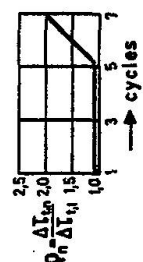


Fig. 18: Bond-stress-relaxation of an initial bond-stress " τ_0 ", may be estimated by means of the expression $\Delta \tau_{t,n} = \rho_1 \cdot \rho_n \cdot \tau_0$



forced concrete elements (especially those related to deformation characteristics of these elements after cracking), the interplay between steel stress σ_s , concrete stress σ_c , local bond stress τ , and local slips along the steel-to-concrete interface is of fundamental significance. Therefore, some models regarding local bond versus local slip relationship are reproduced in what follows.

As far as the **monotonic** loading is concerned, a simplified physical model is first reminded (Fig.14). However, it has to be noted that this constitutive law is not unique along the steel element; near free edges and cracks, a gradual decrease of the critical values of bond stresses and slips is observed and should appropriately be taken into account (see i.a. TASSIOS, 1979).

Cyclic bond actions, according to a physical model of TASSIOS, 1979, may be followed by means of the simple constitutive law shown in Fig.15. A more precise formalistic model is reproduced in Fig.16.

Time effects in bond behaviour (bond-relaxation and bond-slip-creep) may be treated by means of the empirical data shown in Fig. 17 and Fig. 18 (PLAINES, TASSIOS, VINTZÉLEOU, 1982).

2.2.2. Pull-out and push-in models

On the basis of the "element-model" of the previous paragraph, simple algorithms may be written for several cases of embedded axially stressed bars: The length of the bar is divided into a number of parts of sufficiently small length Δx , where the basic relationships of Fig. 19a are repeatedly applied. Boundary conditions are shown in Fig. 19b. Thus, analytical results of "mathematical" pull-out/push-in tests may be carried-out as shown in Fig. 20.

2.2.3. Dowel-bond interaction: Much less advanced models are available for this topic. What follows is only an oversimplified proposal, suitable for any practical interaction-function (see i.a. K. Krishnarayan, 1982)
$$\left(\frac{D}{D_u}\right)^n + \left(\frac{B}{B_u}\right)^n = 1, \quad n = 1 \div 2.$$

Each force, in the absence of the others is mobilised by a corresponding displacement; thus $D = D(s)$ and $B = B(w)$, Fig. 21. A mutual factoring is proposed in order to estimate "interaction values":

$$D_1 \cong D(s) \cdot \left(1 - \frac{w}{w_u}\right), \quad B_1 \cong B(w) \cdot \left(1 - \frac{s}{s_u}\right),$$
 where "s" and "w" are shear and extensional displacements correspondingly. Ultimate values are

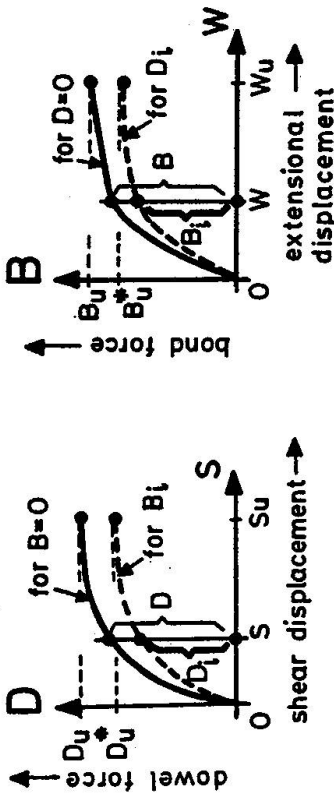


Fig. 21: Dowel-bond interaction hypothesis. In presence of a pull-out forces B_i produced by an extension "w", the dowel force mobilised by a shear displacement "s" is estimated by the expression $D_i = D(1 - \frac{w}{w_u})$, whereas $B_i = B(1 - \frac{s}{s_u})$

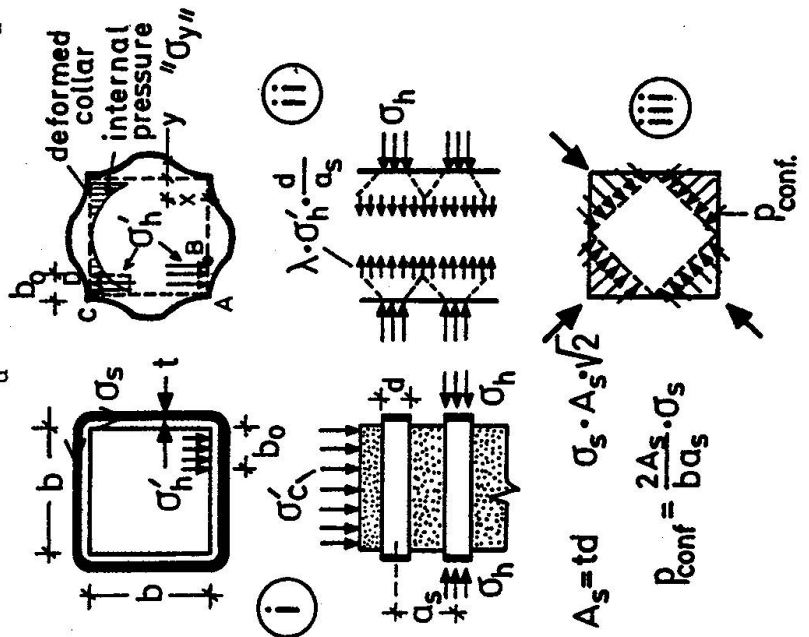


Fig. 22: Mechanics of steel collars (confining action)

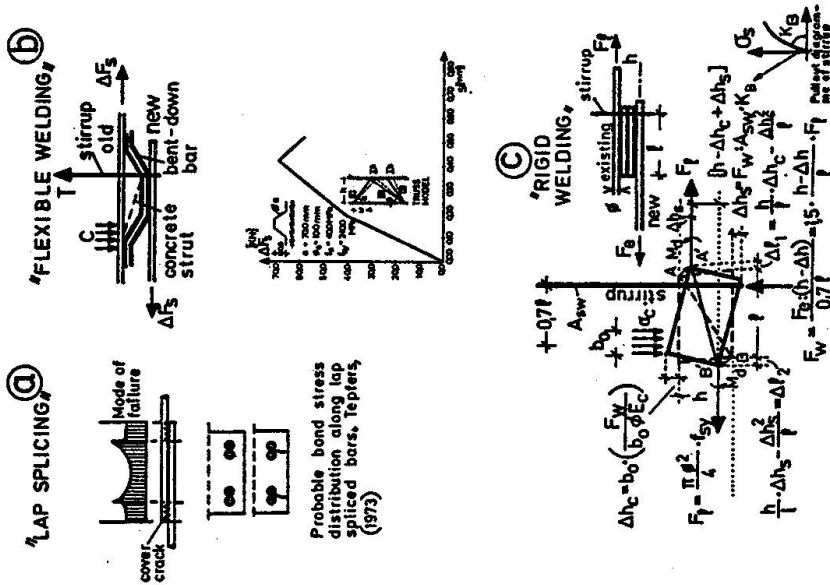


Fig. 23: a) Lap splicing is a complicated mechanism of load transfer through double concrete-to-steel bonding: Average bond strength at the splice length l_s (Orangun, C + 1977): $\tau_u = 0.10 + 0.25 \frac{C}{\phi} + 4.15 \frac{f_{cc}}{f_{cc}} + \frac{A_{s, tr} \cdot f_y \cdot t_f}{420 \cdot \phi}$ where: $\sqrt{f_{cc}}$

C: concrete cover
f_{cc}: concrete compressive strength

A_{s, tr}, f_y, t_f: area of one stirrups' length and yield strength of stirrups

a: stirrups' spacing
b) When the distance between existing and new reinforcement is large, "bent-down" auxiliary bars help fixing; a somehow "flexible" connection is formed. Its analysis is carried out through a simple truss model.

c) A more "rigid" connection is made by means of one or more short auxiliary bars

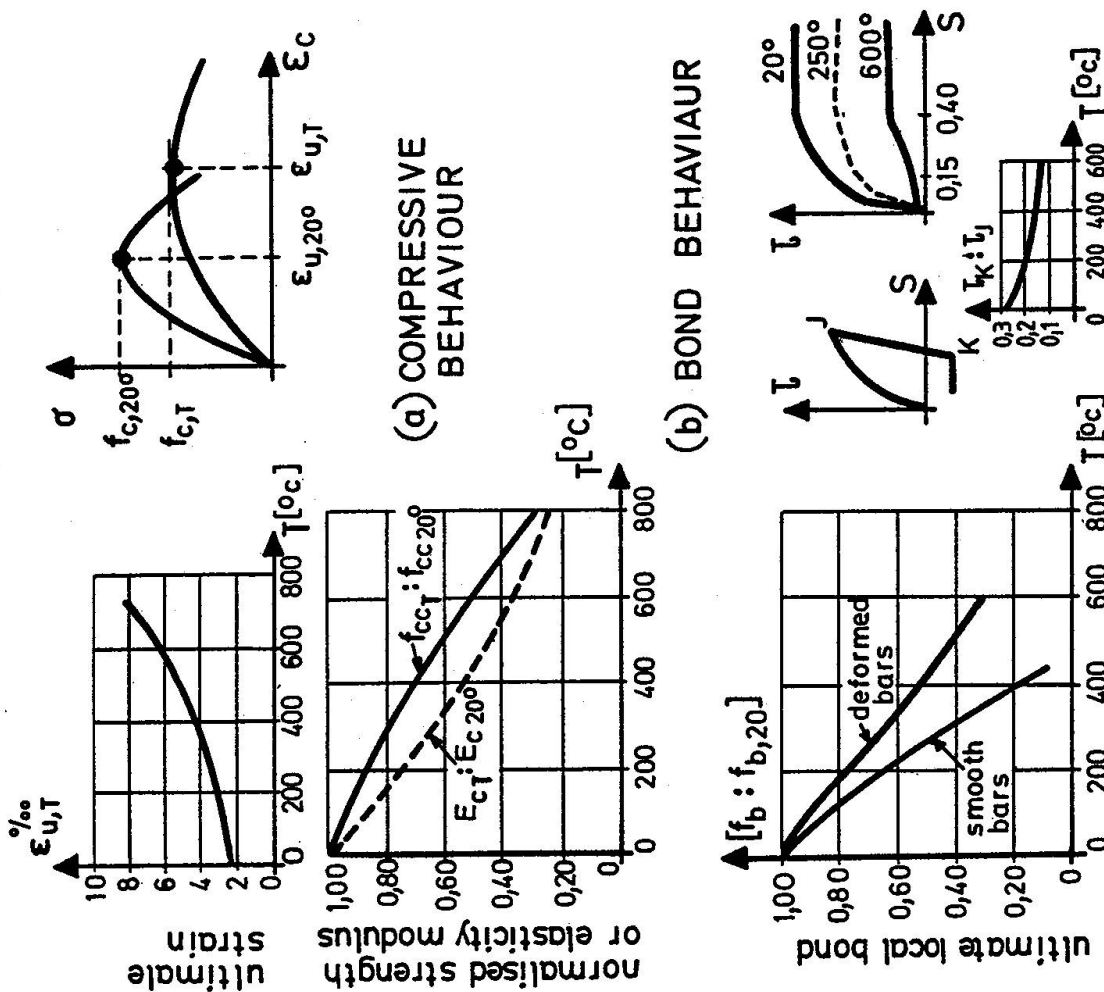


Fig. 24: Concrete after fire: Constitutive laws for compression and bond

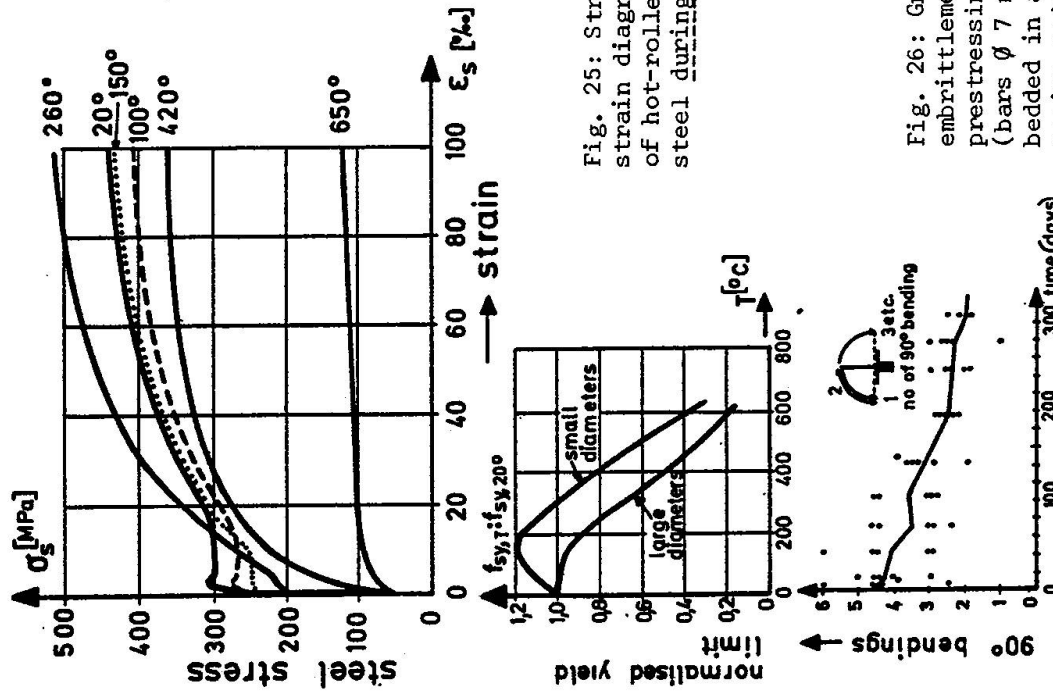


Fig. 25: Stress-strain diagramme of hot-rolled steel during fire

Fig. 26: Gradual embrittlement of prestressing steel (bars ϕ 7 mm) embedded in a corrosive soil.



also factored:

$D_u^* = D_u(1 - \frac{w}{w_u})$, $B_u^* = B_u(1 - \frac{s}{s_u})$. Therefore, the initial interaction function is respected. Nevertheless, it is **not** suggested to apply these rather strong interaction relationships for low values of "D" and "B", (say, lower than one third of the ultimate).

2.3. Confining action

Steel may also indirectly contribute to load transferring when used as a **collar** element. A threefold action may be envisaged: a) Connection of additional longitudinal rolled shapes, b) Shear resistant action, c) Triaxial effects on the confined concrete element.

The confining action of a steel collar may be mobilised by several means:

Differential **Poisson's** deformation due to additional axial stresses σ'_c (acting after taking off of shores). In such a case, the resistance of the collar as a closed frame against horizontal deflections generates horizontal pressures σ'_h (Fig. 22 ii) near the corners. For compatibility of deformations near the edge near (strip ABCD), the following simplified equation may be written

$$v \cdot \frac{\sigma'_c}{E_c} - \lambda \cdot \frac{\sigma'_h}{E_c} \cdot \frac{d}{\alpha_s} = \frac{\sigma_s}{E_s}$$

whereas for equilibrium

$$\sigma_s = \sigma_h \cdot \frac{b_o}{t}$$

Notations are explained in Fig. 22; additionally:

v = Poisson's ratio of concrete

λ = correction factor considering the fact that the strip ABCD is not detached

b_o = effective width where uniform internal pressure is supposed to act; it may be calculated after the analysis of the frame is carried out:

$$y = (v \frac{\sigma'_c}{E_c} - \frac{\sigma_y}{E_c} \cdot \frac{d}{\alpha_s}) \cdot \frac{b}{2}, \quad \ddot{y} = -\frac{bd}{2E_s \alpha_s} \frac{d^2 \sigma_y}{dx^2}, \quad d \cdot \sigma_y = \frac{d^2 M}{dx^2},$$

$$\ddot{y} = \frac{1}{R} = \left[\frac{M}{E_s J_s} = -\frac{b}{2E_s \alpha_s} \cdot \frac{d^4 M}{dx^4} \right].$$

Prestressing of collars may be another means to mobilise its confining action. Initial prestressing value " σ_{s0} " will be reduced (be-

cause of concrete creep " ϕ ") by

$$\Delta\sigma_{SP} = \alpha \cdot \phi \cdot \sigma_{HP}, \quad (\alpha = E_s : E_c). \quad \text{Therefore } \sigma_{HP} \cdot b_o = \sigma_{SP} \cdot t = (\sigma_{SO} - \alpha \phi \cdot \sigma_{HP}) \cdot t.$$

Preheating of collars is another possibility. Compatibility and equilibrium equations in this case are written as follows:

$$\lambda \cdot \frac{\sigma_{HT}}{E_c} \cdot \frac{d}{\alpha_s} \cdot (1 + \phi) \cong \alpha_T (T_o - \Delta T - 20) - \frac{\sigma_{ST}}{E_s}$$

$$\sigma_{ST} = \sigma_{HT} \cdot \frac{b_o}{t},$$

where T_o = initial steel temperature

ΔT = temperature loss up to wedging of the collar

α_T = thermal coefficient of steel.

Due to the final steel stress σ_s a diagonal force equal to $\sigma_s A_s \sqrt{2}$ is applied to each corner. An appropriate friction coefficient $\mu_{s,c}$ (s. §II.3.1) may secure the local transfer of an axial force equal to $\Delta N = \mu_{sc} \cdot \sigma_s A_s \sqrt{2}$ from the concrete element to the longitudinal steel rolled shapes, if provided. Simultaneously, at least half of the cross-section of the concrete element (Fig. 22 iii) is profiting of a triaxial effect, due to a lateral pressure

$$\sigma_x = \sigma_y = \frac{2A_s}{ba_s} \cdot \sigma_s.$$

Finally, additional shear resistance, due to truss-action of the collars, may be mobilised immediately as long as full wedging of these collars is secured. To this purpose, a certain minimum of confinement is necessary.

2.4. Steel to steel load-transfer

For the sake of completeness of the framework of this Report's contents, the structural behaviour of steel-to-steel connections should also be discussed in this chapter. Some of these connections are shown in Fig. 23, together with some simple models describing their structural behaviour. The model "c" needs a brief derivation of an expression for the local lengthening Δl of the joint, due to the straightening tendency of the non-colinear forces F_1 which are transferred from the existing to the new reinforcement (Fig. 23c):

$$\text{Total vertical displacement of the joint } \Delta h = \Delta h_c + \Delta h_s = \left(\frac{1}{\phi E_c} + \frac{1}{A_{sw} K_B} \right) \cdot F_w = \lambda \cdot F_w.$$

$$\text{Force offered by the stirrup: } F_w = 1,5 \frac{h - \Delta h}{1} F_1 = h : \lambda \left(1 + \frac{1}{1,5 \lambda F_1} \right).$$

$$\text{Total "lengthening": } \Delta l = \Delta h \cdot \frac{h}{1} - \frac{1}{1} \left[\Delta h_s^2 + \Delta h_c^2 \right].$$

$$\text{Therefore } \Delta l \cong \frac{h^2}{21} \cdot \left\{ \left[4\alpha\beta + 1,3 \frac{1}{F_1} (\alpha + \beta) \right] : \left[(\alpha + \beta) + 0,7 \frac{1}{F_1} \right]^2 \right\} = \xi \cdot \frac{h^2}{21},$$

$$\alpha = \frac{1}{\phi E_c}, \quad \beta = \frac{1}{A_{sw} K_B}.$$



3. ALTERATIONS OF CONSTITUTIVE LAWS DUE TO NON-MECHANICAL ACTIONS

Damage or weakness due to environmental actions may drastically modify the constitutive laws of structural materials. Assessment of structures cannot be realistically carried-out without full knowledge of these modifications.

In Fig. 24 and 25 experimental data are reproduced, concerning alterations of materials' behaviour due to **fire**.

Some data are presented in Fig. 26 concerning consequences of **corrosion**.

The subject, inspite its great practical importance, cannot be considered as sufficiently covered by available information.

4. COMPOSITE MODELS

Sofar, individual-models have been considered, regarding interface load transfer through a specific material, under specific conditions. This chapter is devoted to some models concerning load transfer through several materials and several mechanisms simultaneously.

4.1. Shear through crack

The kinematics of such a composite model and its force response are dependant on the micro-geometry of the crack faces (or, more generally, of the interface). As a matter of fact, this geometry is of a very stochastic nature and it is bound to be modified during the loading itself; therefore it can never be realistically predicted or reproduced. Nevertheless, several simplified geometrical forms of interfaces may be investigated, in order to build-up a structural model numerically inaccurate but physically sound. Its subsequent calibration (by means of experimental data and or numerical parametric studies) will produce predictions of a much larger validity and broader applicability than any formalistic empirical model.

A rational crack-face morphology (parabolic segments) has been studied by FARDIS, BUYUKOZTURK, 1979, leading to a direct expression of the shear force transmitted between two concrete blocks, separated by a crack. External bending moment and axial force are known; all mechanisms of shear transfer were supposed to react elastically. In what follows here, a simpler crack-force geometry is considered in order to facilitate a **more general** modeling of all load-transfer

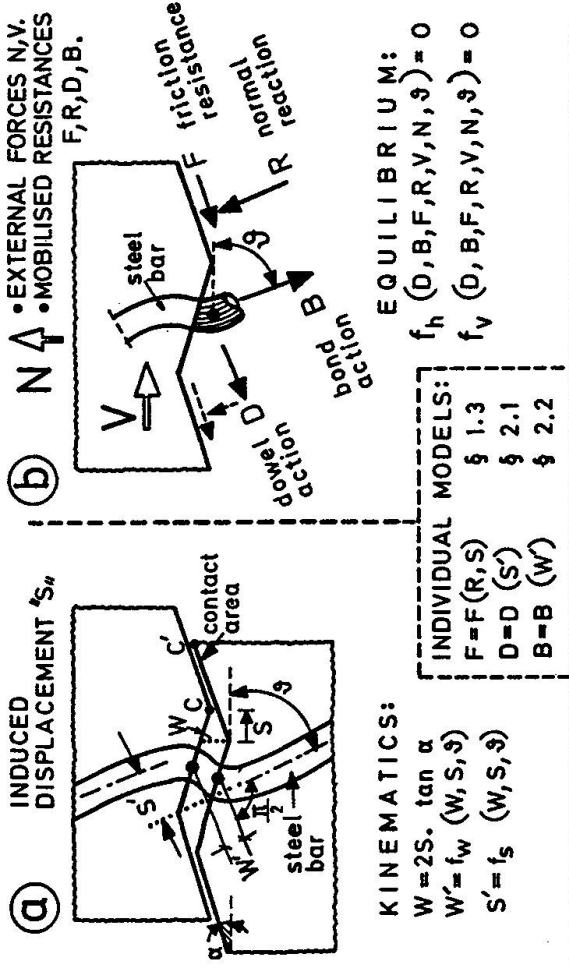


Fig. 27: Shear deformation (displacement "s") is imposed to a one-side-closed crack through "q" R.C. section: Reactions of three mechanisms are mobilised (friction dowel and bond)

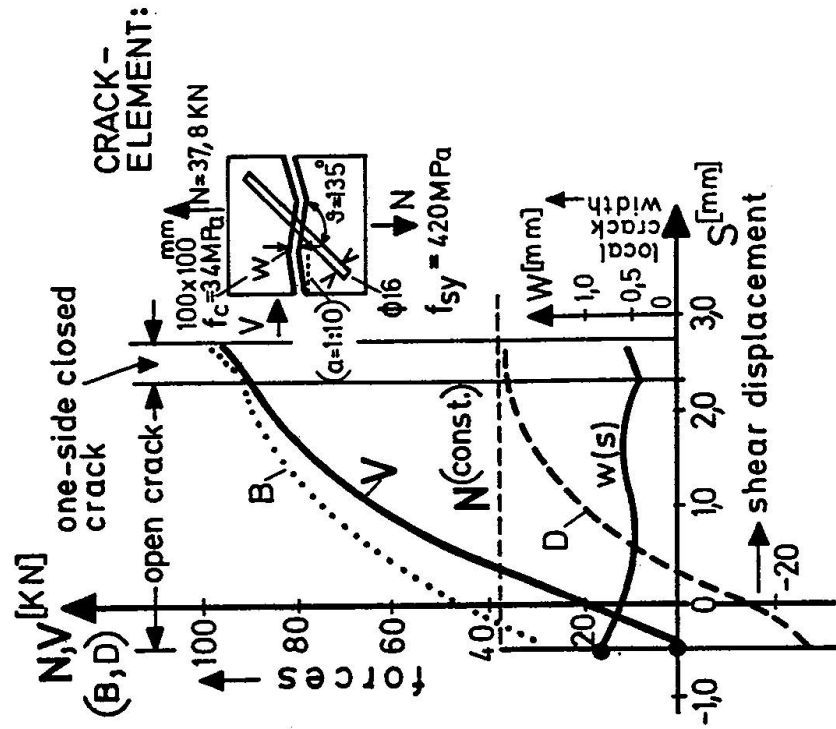


Fig. 28: Shear deformation (displacement "s") is imposed to an open crack through a R.C. section (previous crack width "w"): Reactions of two mechanisms are mobilised (dowel and bond).

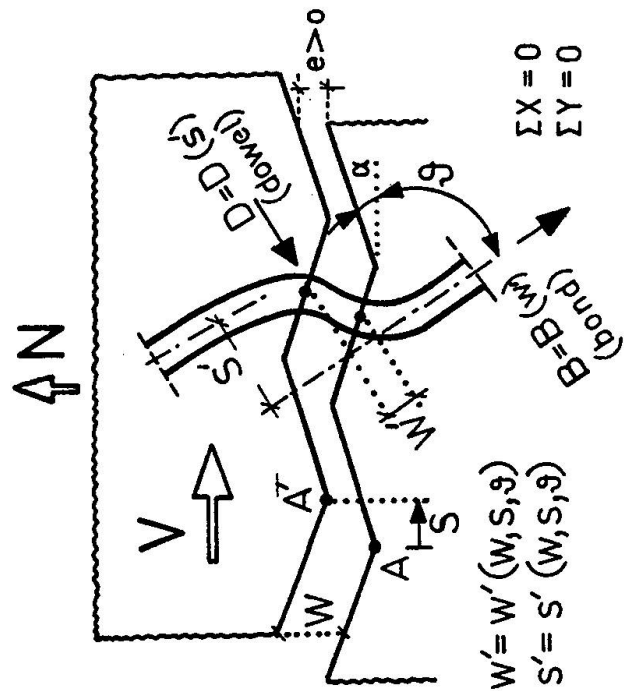


Fig. 29: A numerical application of the composite "shear-through crack" model, TASSIOS, SCARPAS, 1982



mechanisms, being taken into account with their non-linearity and their actions' - history dependence. Inclined linear segments forming an interface were initially considered by P. and H. BIRKELAND, 1966 (and were also taken into account by TASSIOS, TSOUKANTAS, 1978, in modeling large precast panels' connections). Deformations of these asperities are not considered at this stage.

The interface is crossed by steel bars of arbitrary direction, diameter and spacing. A **crack-element** of a given small length is considered. First, a closed crack is examined (Fig. 27a); a shear displacement "s" is imposed along its plane and a local opening "w" = $2s \tan \alpha$ is proposed. As a consequence, transverse reinforcements are submitted to a local extension "w'" and a local kinking "s'", both expressed as functions of the imposed displacement "s" (and the angles "α" and "θ"). Correspondingly a bond reaction "B" and a dowel reaction "D" are mobilised which, together with the friction force "F" (and the normal reaction "R") along the contact area cc' of the crack-face, constitute the r e s i s t a n c e s of the crack-element considered.

Given an "s"-value, the kinematic parameters "w'" and "s'" are fully determined. Therefore, the steel reactions D and B are also fully determined (s.§2.1 and 2.2). For the friction force F (s.§1.3) the value of the normal force R would also be needed, in order to select the appropriate constitutive curve (τ, s) for a specific value of normal concrete stress. Consequently, in the two equilibrium equations (Fig. 27b) remain three unknowns. Nevertheless, the crack-element considered belongs to a general crack of a building-element. Therefore, due to the i n c r e m e n t a l shear displacement applied here, the "external" local forces V and N acting on the crack-element cannot variate independently; a relationship $f(\Delta V, \Delta N) = 0$ does exist in every specific case (e.g. $N=0$ or $\Delta V = \Delta N$, etc).

Thus, for a given shear displacement, incrementally imposed to a crack-element, its **response** is fully determined, provided that a positive value for the reaction R is found.

Otherwise, a fully open crack should be considered in the next step (Fig. 28), starting by an initial value w_0 . In this case, for the subsequent increment of displacement "s", the kinematic data "w'" and "s'" contain an additional unknown which is the new crack-width "w" (now not submitted to any geometrical restriction as a function of "s"). Therefore, in the two equilibrium equations, three unknown are again present; the additional condition $f(\Delta V,$

$\Delta N) = 0$ will complete their determination.

As a consequence, the response of every in-plane cracked R.C. system may be fully defined step by step as a function of the shear displacement. Fig. 29 gives an example of application of the above model; any "sub-model", so to say, expressing the behaviour of each load-transfer mechanism, may be used as an input of this composite model.

Relatively little sensitivity has been observed for angle " α "-values varying between 1:5 to 1:15.

A somehow similar application may be seen in Fig. 48.

4.2. Shear through glued plates

In the oversimplified model of Fig. 30, a part of the glued sheet, corresponding to an inclined shear-crack, is undertaking the shear force V_w transferred through web. The distribution of the adhesive stresses " τ_{gl} " along the height of the sheet may be found by means of the model presented in §2.2.2, where a constitutive law like that shown in Fig. 5b will be taken into account.

However, for design purposes a rough approximation of the mean value $\bar{\tau}_{gl}$ could be sought (Fig. 30), e.g. $\bar{\tau}_{gl} = 0,4f_b$, so that the thickness of the sheet " t " and the bond strength " f_b " needed should fulfill the following conditions (which, of course, must be completed by the appropriate partial safety factors):

$$t > 0,4l_o \cdot \frac{f_b}{f_{sy}}, \quad f_b > 2 \cdot \frac{V_w}{d l_o}$$

Part II: Remodeling of Building-Elements (for assessment and redimensioning)

1. BEAMS AND SLABS

Stiffness after damage may be assessed first by means of empirical data like those presented in Fig. 31. Formalistic models may also be used, like those proposed by THOMPSON, PARK, 1975; an example is given in Fig. 32. Fully analytical models may be built-up on the basis of the fundamental data presented in Part I.

After-repair stiffness K_r , as a percentage of the stiffness K_m of the repaired or strengthened section as if it were monolithic,

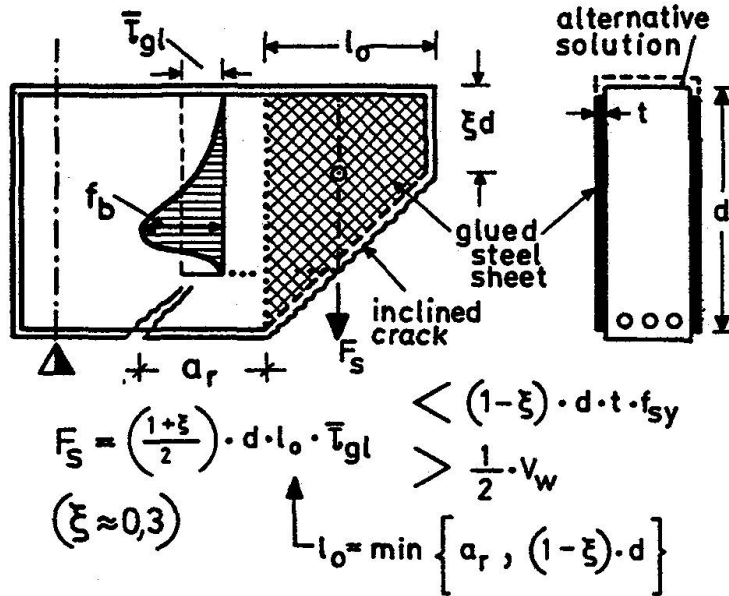


Fig. 30: An oversimplified model for shear-force transfer through epoxy-resin glued steel sheet.

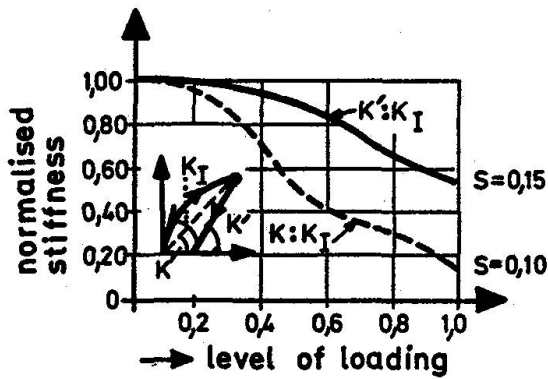


Fig. 31: Empirical values for residual stiffness after damage. A scattering equal to $\pm s$ should be taken into account

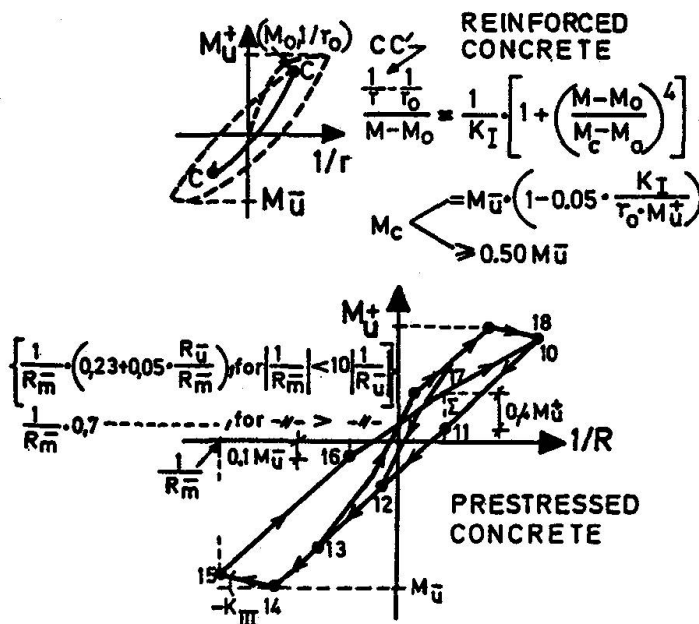


Fig. 32: Formalistic models (Thompson, Park, 1975) for cyclic bending

may be estimated by means of empirical data (e.g. Fig. 33) or may be calculated by means of a simplified analytical model. There are two causes of interface slip (s. Fig. 34), between existing section "1" and additional section "2":

a) Shear stresses $\tau_{1,2}$ at the interface are transferred by adhesion (§I.1.2); a corresponding slip $s = \tau_{1,2} : k$ will take place, where $k \approx 10 \div 20 \text{ KN/mm}^3$ (s. Fig. 5). Referring to Fig. 34, the following equation may be written:

$$\text{Monolithic rotation} \quad \frac{d\theta_m}{dx} = \frac{1}{r_m} = \frac{M_Q}{K_m}.$$

$$\text{Final rotation (after slip)} \quad \frac{d\theta_r}{dx} \left(= \frac{d\theta_x + \Delta d\theta}{dx} \right) = \frac{1}{r_r} = \frac{M_Q}{K_r}$$

$$\therefore K_r : K_m = 1 : \left(1 + \frac{\Delta d\theta}{d\theta_x} \right),$$

where $d\theta_m = \epsilon_{s1} \cdot dx : (d_1 - x_Q)$, $\epsilon_{s1} = \sigma_{s1,Q} : E_s$, $s = \tau_{1,2} : k$

$$\Delta d\theta_o = S : (d_1 - x_Q + x_Q \cdot d_2 / d_1), \quad \tau_{1,2} \approx V_Q : b_o \cdot j.$$

b) Straightening of the non-linear connection between existing and additional reinforcement, according to the model shown in §I.2.4 (Fig. 23c), create an additional "strain" of the tensioned fibre. If l_a is the distance between consecutive points of welding, this additional strain is equal to

$$\Delta \epsilon_s = \frac{\Delta l}{l_a} = \xi \cdot \frac{h^2}{l l_a}, \text{ where } \xi = \xi \left(\frac{1}{\phi E_c}, \frac{1}{A_{sw} K_B}, 1, F_1 \right) \text{ see §2.4.}$$

(The stiffening effect of dowel moments has been neglected).

In this expression (see also Fig. 34):

h, l = height and length of the welding joint

A_{sw} = new stirrup's cross-section, corresponding to each additional bar

K_B = pullout stiffness for the stirrup (see §I2.2.2).

ϕ = the diameter of the bars of existing reinforcement

F_1 = the additional tensile force to be transferred to each new steel bar at the welding joint considered.

Therefore, neglecting the additional concrete strain which corresponds to this $\Delta \epsilon_s$, one could write:

$$\frac{1}{r_m} = \frac{\epsilon_s + \epsilon_c}{d} = \frac{M_Q}{K_m}, \quad \frac{1}{r_r} = \frac{\epsilon_s + \Delta \epsilon_s + \epsilon_c}{d} = \frac{M_Q}{K_r}, \quad K_r : K_m \approx 1 + \frac{\Delta \epsilon_s}{\epsilon_s + \epsilon_c},$$

where ϵ_s and ϵ_c are known quantities from the dimensioning of the composite section as monolithic.



Fig. 34: Strengthened flexural member. A horizontal slip is taking place under the influence of the shear stress $\tau_{1,2}$.

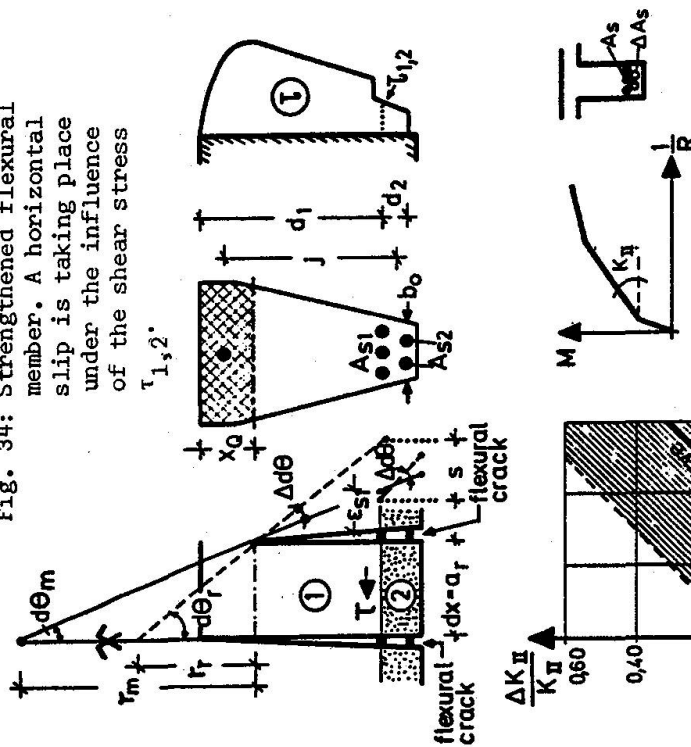


Fig. 33: Normalised differences between experimental and computed values of stiffness after cracking VASSILIU, 1974

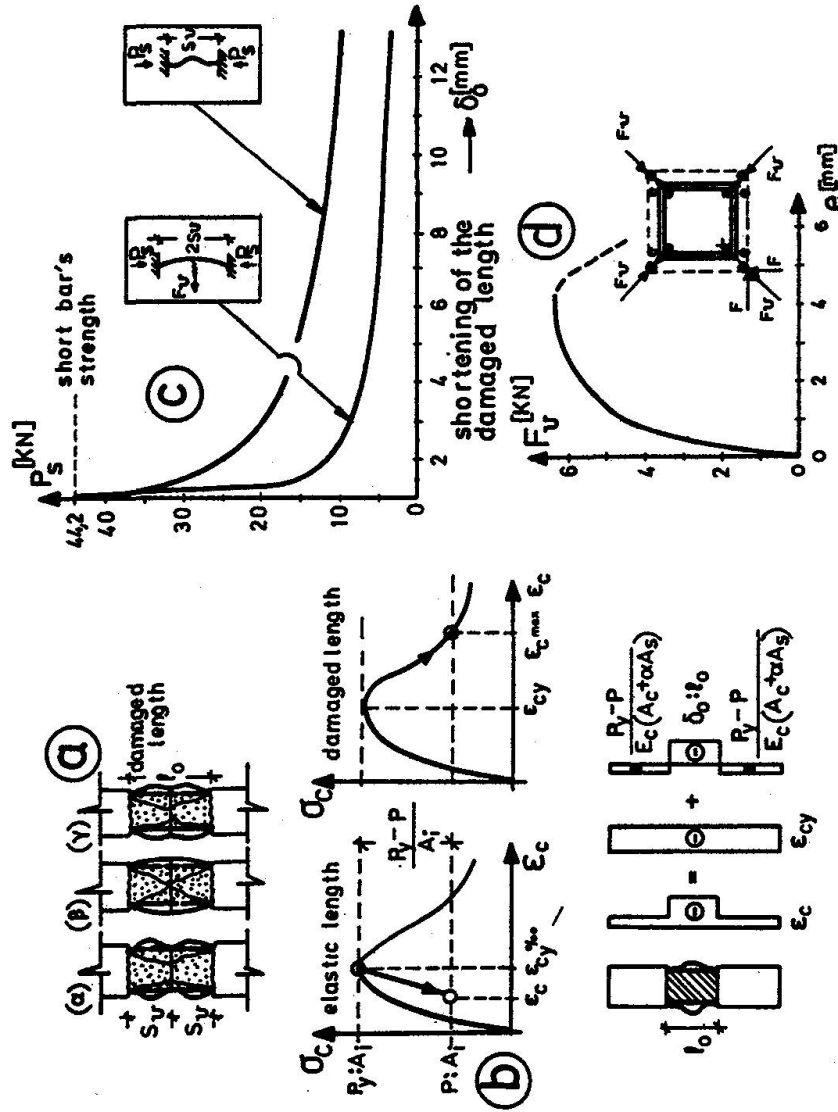
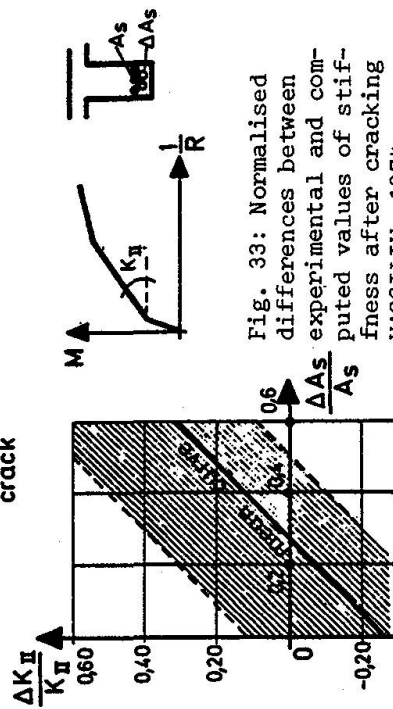


Fig. 35: A computational model for the evaluation of post-plastic deformations of a damaged, axially loaded, column.

Strength of cross-sections after damage may be evaluated by traditional models based on materials' sub-models presented in Part I. Nevertheless, based on experimental findings, a more simple design method may be used, under certain limiting conditions: Re-dimensioning may be carried-out taking into account the entire section, constituted both of the old and the additional materials, as if the final section were monolithic. Obviously, such a hypothesis leads to strength and stiffness characteristics ($M_{u,m}$, $V_{u,m}$, K_m) higher than the real ones ($M_{u,r}$, $V_{u,r}$, K_r). Corresponding correction factors " γ_n " are foreseen by the Greek "Recommendations for Repair", as follows, provided that appropriate specifications and detailing rules are met:

Epoxy glued plates: $\gamma_n' = 1$, provided that $\Delta M_{u,add} < 0,5.M_{u,exist}$.
Concrete cast on top and/or on sides (~~together~~ with additional welded steel bars)

$$\text{when } \Delta A_c < \frac{1}{3} A_c$$

$$\text{when } \Delta A_c > \frac{1}{3} A_c$$

$$M_{u,r}:M_{u,m} = \begin{matrix} 1,0 & \text{for slabs} \\ 0,8 & \text{for beams} \end{matrix}$$

$$M_{u,r}:M_{u,m} = 0,65 \text{ for beams}$$

$$V_{u,r}:V_{u,m} = 0,8 \text{ for beams}$$

Shotcrete (plus additional welded steel bars)

$$M_{u,r}:M_{u,m} = \begin{matrix} 1,00 & \text{for slabs} \\ 0,80 & \text{for beams} \end{matrix}$$

$$V_{u,r}:V_{u,m} = 0,80 \text{ for beams}$$

Joints repaired by means of external collars or bands

$$\Delta V_{u,r}:\Delta V_{u,m} = 0,5.$$

2. R.C. COLUMNS

2.1. Residual characteristics

Axially loaded columns are considered here first. If the damage is not caused by an (over) loading, residual characteristics may be evaluated directly by means of the altered constitutive laws (e.g. §13). Yet, buckling critical load of columns is not proportionally influenced, unless the damage is located near their critical length (central third of the equivalent buckling length). In case of a mechanical cause of damage, taking into account a pathological image as shown in Fig. 35a, one should consider two sources of residual bearing capacity after concrete's yield: Concrete's response along the descending branch of its " σ - ϵ " diagramme (Fig.35b), and naked steel bars' resistance before their complete buckling (Fig.35c).



Fig. 36: Post-plastic deformations of a damaged axially loaded, column.

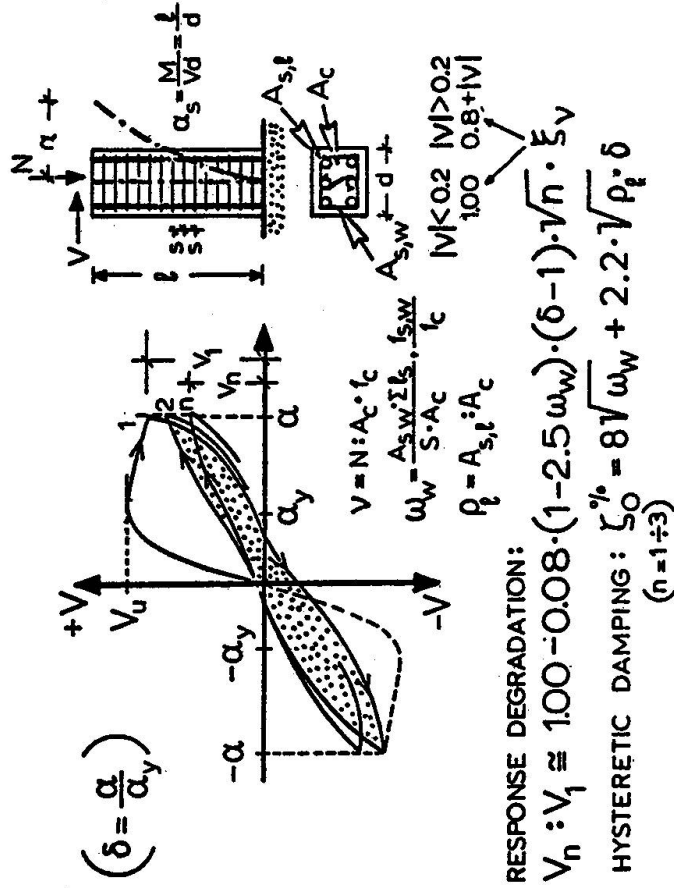
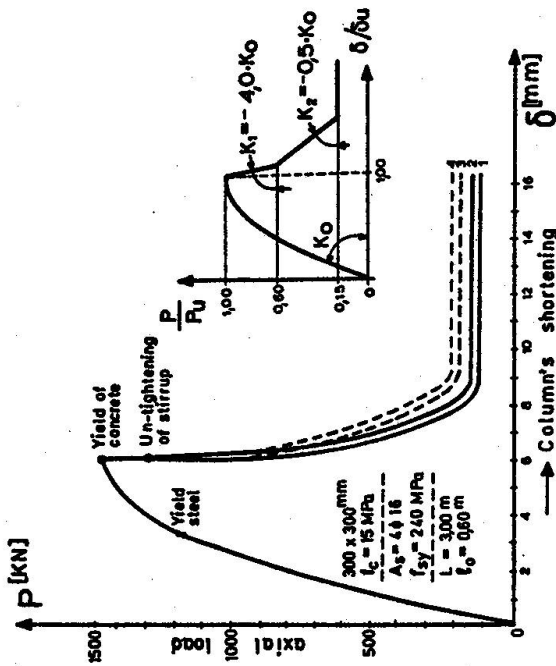


Fig. 37a: Response degradation and hysteretic damping of R.C. columns seismically damaged, when their cyclic deflection "a" and the number of full cycles "n" are estimated, (TASSIOS, GRISPOS, 1982)

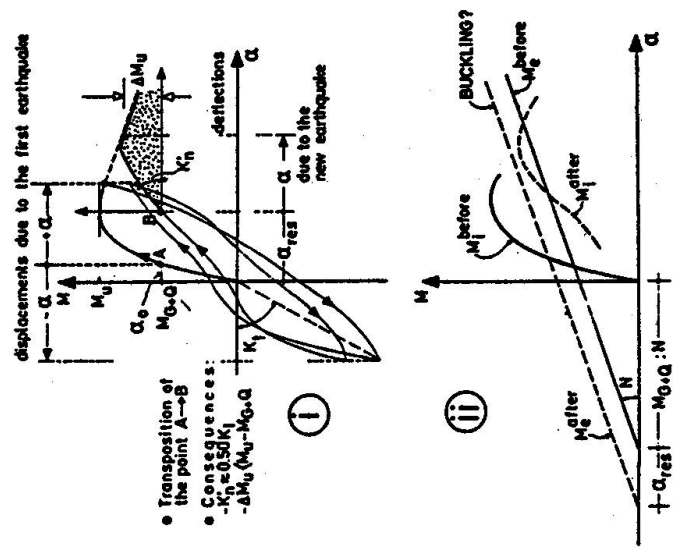


Fig. 37: Assessment of a R.C. column damaged by an earthquake

In this connection the confining action of the stirrup (Fig. 35d) is of a basic significance.

Thus, following-up the gradual increase of column's shortening, FROUSSOS and TASSIOS, 1982, have found theoretically post-yield force displacement relationships shown in Fig. 36, depending on the buckling mode of longitudinal bars and the percentage of concrete's cross-section popped-out during the process.

Laterally loaded columns, especially after damage produced by an earthquake, may be assessed if the data represented in Fig. 37i are previously known: "unexpected" displacement " α " and residual displacement " α_{res} ". Models discussed in §I.4.1 may be used in order to predict stiffness K'_n , versus a possible new loading, and available moment capacity ΔM_u .

Fig. 37ii illustrates a simple method of checking possible instability conditions created after damage (M_e , M_i denote externally applied moments and internal moments mobilised by the imposed deformations).

Finally, empirical formulae predicting response degradation (when some data on deflections caused by an earthquake are available) may be practically useful in assessing seismically damaged columns (Fig.37a).

2.2. Jacketing

A R.C. jacket is shown in Fig. 38a, together with several "load transfer paths" (Fig.38b). Number "3" and "5" mechanisms are included in the model of the previous paragraph, whereas number "4" cannot be reliable at all. Therefore, mechanisms "1" and "2" will be considered here. Load-transfer sub-mechanisms are to be expressed in terms of **slip** between column and jacket, which gradually mobilises each mechanism. Finally, for each value of column slip, superposition of all forces undertaken by each mechanism will be carried out.

- (i) Load-transfer " T_s " between original and new longitudinal reinforcements (s.§I2.4, Fig.23a).
- (ii) Dowel actions " T_d " at the legs of the bend-down bars (comp.§I2.1).
- (iii) Concrete to concrete friction forces, due to differential Poisson-effect (comp.§I2.3).

Referring to Fig.39, the following equations may be written for the simpler case when no load at all can be transferred by the damaged section $x = 0$:

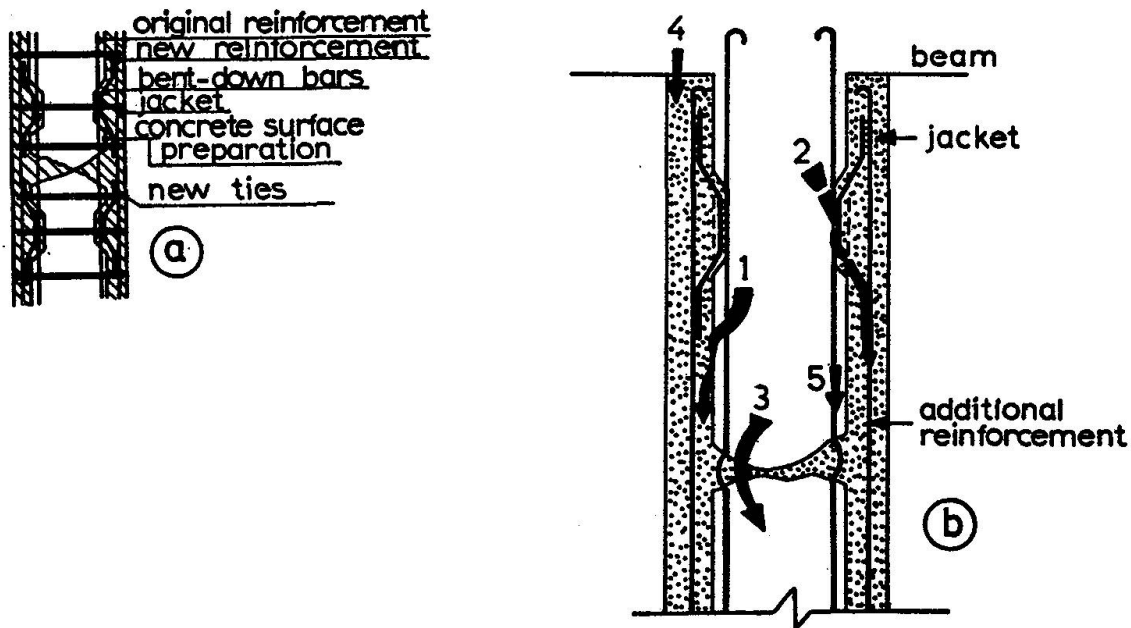


Fig. 38: a) Typical column repair by means of a concrete jacket
b) Load Transfer Mechanisms

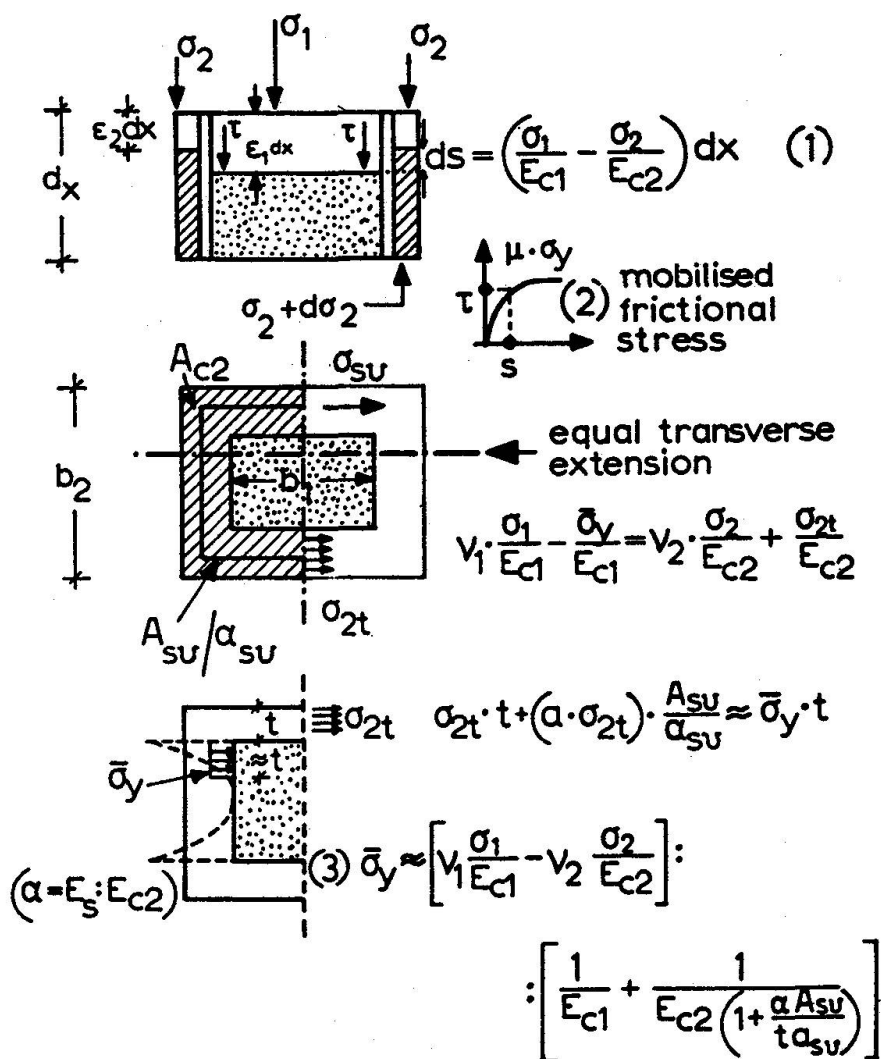


Fig. 39: Shearing and normal stresses developed at the "jacket/original column" interface

$$s_x = s_o + \int_0^x \left(\frac{\sigma_1}{E_{c1}} - \frac{\sigma_2}{E_{c2}} \right) dx \quad (1)$$

$$\tau_x = f(s_x, \bar{\sigma}_y), \quad (\text{Fig.6}) \quad (2)$$

$$\bar{\sigma}_y = \left[v_1 \cdot \frac{\sigma_1}{E_{c1}} - v_2 \frac{\sigma_2}{E_{c2}} \right] : \left[\frac{\sigma_1}{E_{c1}} + \frac{1}{E_{c2} \left(1 + \frac{\alpha \cdot A_s}{t \alpha_{s,i}} \right)} \right] \cdot f_{ct} \quad (3)$$

$$\sigma_2 = \left[\sum_{\alpha \rightarrow x} (T_d)_i + \int_x^{\alpha} \tau_x \cdot 8t \cdot dx \right] : A_{c2} \quad (4)$$

$$(T_d)_i = \psi(s_x), \quad (\text{Fig.12}) \quad (5)$$

$$\text{total } T_s = \sum_{\alpha \rightarrow x} (T_s)_i, \quad T_s = z(s_x), \quad (\text{Fig.5}) \quad (6)$$

$$(\sigma_1 A_{c1} + \sigma_2 A_{c2} + \text{total } T_s)_x = N. \quad (7)$$

The above system of equations has a solution at every cross section along the column (7 unknowns at each x-section) as well as at the $x=0$ x-section where $\sigma_{1,0} = 0$. It can be solved by trial and error, although double convergence problems have to be solved. Fig. 40 gives some results of this model (TASSIOS, 1982). Similar methods may be used in the case of repair by means of large rolled-shapes fixed on the four corners of a damaged column through preheated collars (comp. § I.2.3).

2.3. External collars

External collars are used mainly when ductility increase is the principal aim of R+S. Nevertheless, shear (and sometimes axial) strength may also be favourably influenced by these additional hoops, (s. § I.2.3 and Fig. 22).

There is experimental evidence (i.a. ARAKAWA, 1980) that for columns reinforced with deformed bars, additional hoops firmly fixed to the columns have the same strengthening effect like hoops initially incorporated in the column; obviously, extra thicknesses are requested to counterbalance construction needs and possible durability effects. Therefore, models predicting ductility of monolithic columns as a function of transversal reinforcement (e.g. Sheikh, Uzumeri, 1979-80), apply in this case too.

3. INFILLED FRAMES

3.1. Shear behaviour of infills

Due to the complexity of the structural system examined in this chapter, formalistic models regarding relationships of shear stress " τ "

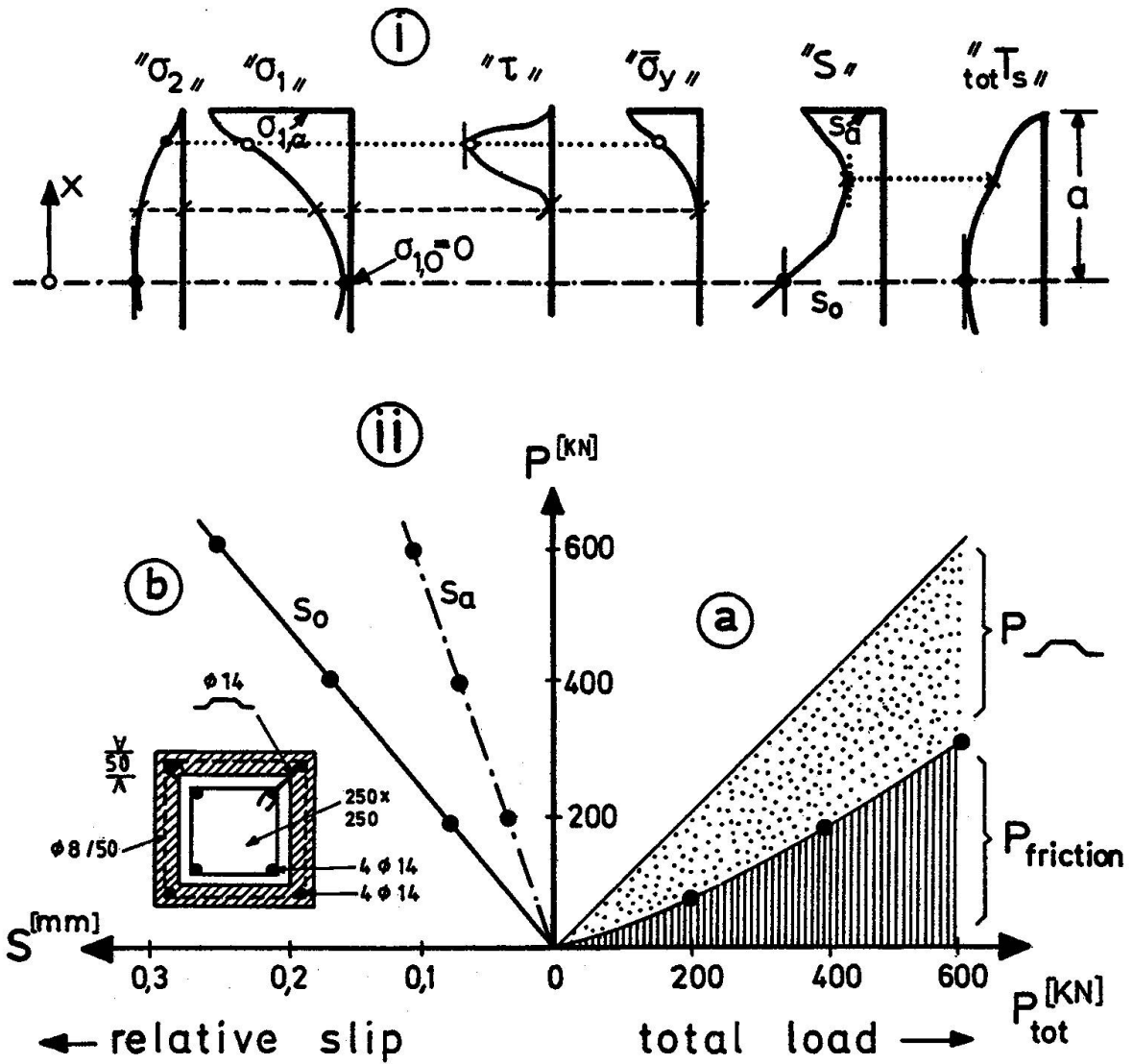
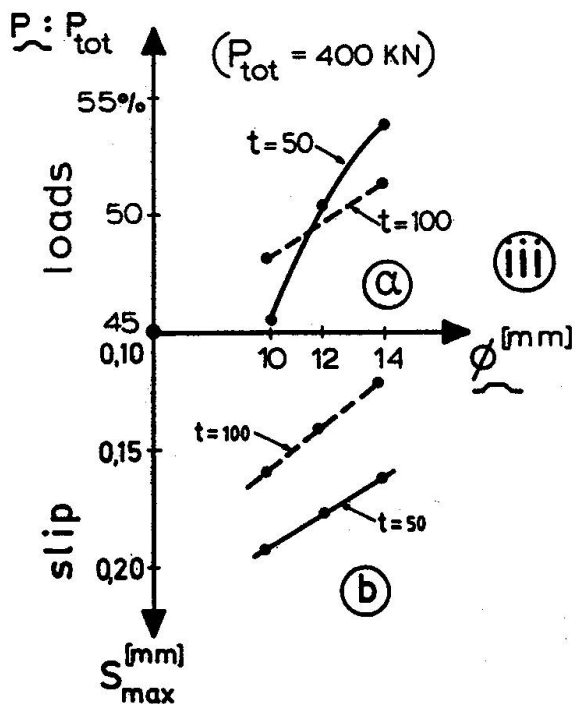


Fig. 40: Load transfer through R.C. jackets of damaged columns: i) Stress and deformations distribution along a jacket of length $2a$, ii) Computed results: load distribution and slips, as a function of loading, iii) The role of the diameter of the bend-down bars



to angular deformation " γ ", would be of a considerable practical importance in modeling infill frames.

Masonry infills exhibit a " τ - γ " behaviour similar to that shown in Fig. 41; a very large scatter is expected due to the large variety of materials, construction techniques and testing methods.

R.C. infills' behaviour may also be roughly predicted by similar diagrammes, although physical and analytical modeling would be easier in this case (comp.§II.4).

3.2. Diagonal strut

One of the most simple models of the composite action of a masonry infill is an idealised diagonal bracing strut, having a width " b_w " (Fig.42), which leads to the same horizontal displacement of the infilled frame, (TASSIOS, 1980).

A more elaborated approach is used by SMITH (1969), calculating the lengths of contact between infill and the legs of the frame near the compressed corners. Based on Smith's experimental findings, one could also approximate strut's width by means of the expression $b_w \approx 0,1.L.\sin 2a$ (s.Fig. 43 for notations).

MAINSTONE (1971) has also valued this width as

$b_w = 2l \cos a = \lambda (h^4 E_w t_w \sin 2a : E_c J_f h)^{-\mu}$ where " λ " and " μ " denote constants and J_f is an average inertia moment of the frame. Practically, for brickwork infills Mainstone suggested $b_w \approx 0,2.L.\cos^2 a$.

Finally, YAMADA et al. (19), for R.C. infills at their maximum capacity, have estimated

$$\frac{b_w}{L} = \frac{\tau_u}{f_{cc}} + \rho_w \cdot \frac{f_{sy}}{f_{cc}} \cdot \sin 2a$$

where $\tau_u \approx 0,2f_{cc}$, shear strength of plain concrete

ρ_w = web steel ratio (equal in both horizontal and vertical direction).

The considerable differences observed between these (and several other) proposals are less important than the physical differences due to quality of materials and workmanship. However, the strut model should not be used but only in modelling linear behaviour of the system; for strength predictions, such a model is not reliable.

3.3. Further analysis

A less simplified approach is needed in case of more engineered infills (like R.C. infills connected to the frames by means of bolts). **Finite elements** is possibly the most powerful modeling method for such a composite building element. Based on the sub-models of:

- Material behaviour (Fig. 41)
- Friction between concrete and mortar (comp. Fig. 6).
- Linear finite elements modeling of the frame itself,

A finite elements model of an infilled frame may easily be built-up.

MALLICK et al.(1967) and STORM (1973) have applied this method, both for static and dynamic loading.

Compatibility between deflections of frame's legs and infill's diagonal strips of two directions, is another principle developed by YAMADA et al. (1974) for R.C. infills. (Fig. 43).

It is interesting to reproduce here a set of experimental results (SUGANO, 1981) regarding the overall behaviour of a R.C. frame infilled with several materials and techniques, compared to the behaviour of the same frame monolithically cast with a R.C. wall (Fig.43b). The experimental finding that strength and ductility are complementary,

$$\left(\frac{V_u}{V_{u,m}}\right) \cdot \left(\frac{\gamma_u}{\gamma_{u,m}}\right) \approx 1, \quad \text{is worth to be noted.}$$

3.4. Dimensioning

Using one of the previously described models of the composite action of infilled frames, the shear and axial forces acting on shear connectors may be calculated; similarly, forces transmitted within the body of the infill are determined. Nevertheless, under some conditions another oversimplified model may also be used for dimensioning, taking care for the appropriate partial safety factors. Fig. 44 is a schematic presentation of this model; several **conservative** situations are alternatively considered (see Fig.44 for notations).

a) The infill is fully wedged: The compressive behaviour of its main diagonal strut (width " b_w ", §3.2) should be secured. Therefore

$$\gamma_n \frac{N}{b_w t_w} = \gamma_n \frac{V_w L}{l_w b_w t_w} < \frac{1}{\gamma_m} f_{cc} \quad (a)$$

where " γ_n " and " γ_m " denote partial safety factors taking care of the inaccuracy of the model and the quality of infill material, respectively.

b) The infill is acting with its three sides not wedged: Now, tension forces "P" are required for equilibrium. Consequently, both infill's horizontal edges and the shear connectors have to withstand "P". I.e.

$$\gamma_n P = \gamma_n \frac{2h_w}{l_w} V_w < \frac{1}{2} n B_{u,conn.} : \gamma_m \quad (b_1)$$



Of course, for the same extreme case, the horizontal force H_w must be entirely transmitted to the infill through shear connectors at the upper interface:

$$\gamma_n V_w < n \cdot D_{u,conn.} \quad (b_2)$$

Interaction should be appropriately taken into account (§I.2.2.3) when estimating $B_{u,conn.}$ and $D_{u,conn.}$.

c) The nominal shear stress $\tau_d = \gamma_n V_w : l_w t_w$ has to be safely taken by the body of the infill. Web reinforcement may be calculated by means of the simple friction model, foreseen in the seismic Annex of the CEB-FIP Model Code (§11.6.5.2.3).

d) The total shear force "V" to be taken by the infilled frame, may be splitted into V_f and V_w , as a function of a common angular deformation " γ ", on the basis of the corresponding constitutive laws (Fig. 44d).

A **calibration** of this oversimplified model is needed before it is used in design.

The bearing capacity of short tensile anchors with anchorage head (Fig. 45) is governed either by the tensile failure of the steel itself or by the pull-out strength of a conical failure surface through the concrete.

Failure governed by steel: $P_s = A_s \cdot f_{sy}$

A_s : nominal cross-section of unthreaded anchor shank, or effective tensile stress area of threaded anchor shank

f_{sy} : specified minimum yield stress or $0,9 f_{su}$ in the absence of a clearly defined yield point.

f_{su} : specified minimum ultimate strength

Failure governed by concrete: $P_c = \pi \cdot l(1+d_h) \cdot f_{ctm}$

f_{ctm} : mean tensile strength of concrete

l : embedment length

d_h : diameter of anchor head

A " γ_n " factor equal to 0,65 is suggested for design purposes.

The following expression may be used for small edge distances

$$P'_c = P_c \cdot \left(\frac{\text{Projected area of partial cone}}{\text{Projected area of complete cone}} \right).$$

4. R.C. WALLS and DIAPHRAGMS

4.1. Residual characteristics

If a complete model for R.C. structural wall is available, it would also be used for a R.C. wall's assessment after damage. E.g. in the

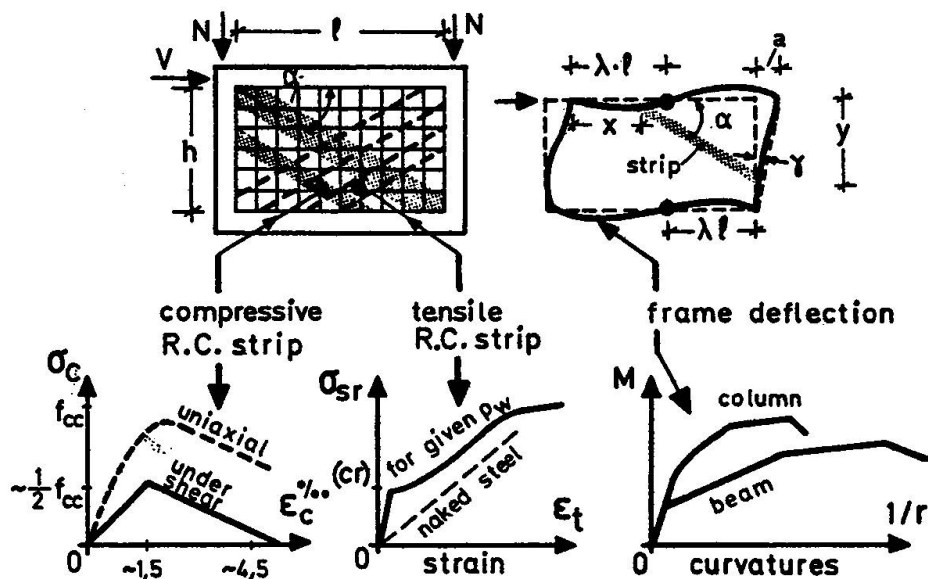


Fig. 43: Composite action of R.C. frame and R.C. infill wall, according to YAMADA et al., 1974.

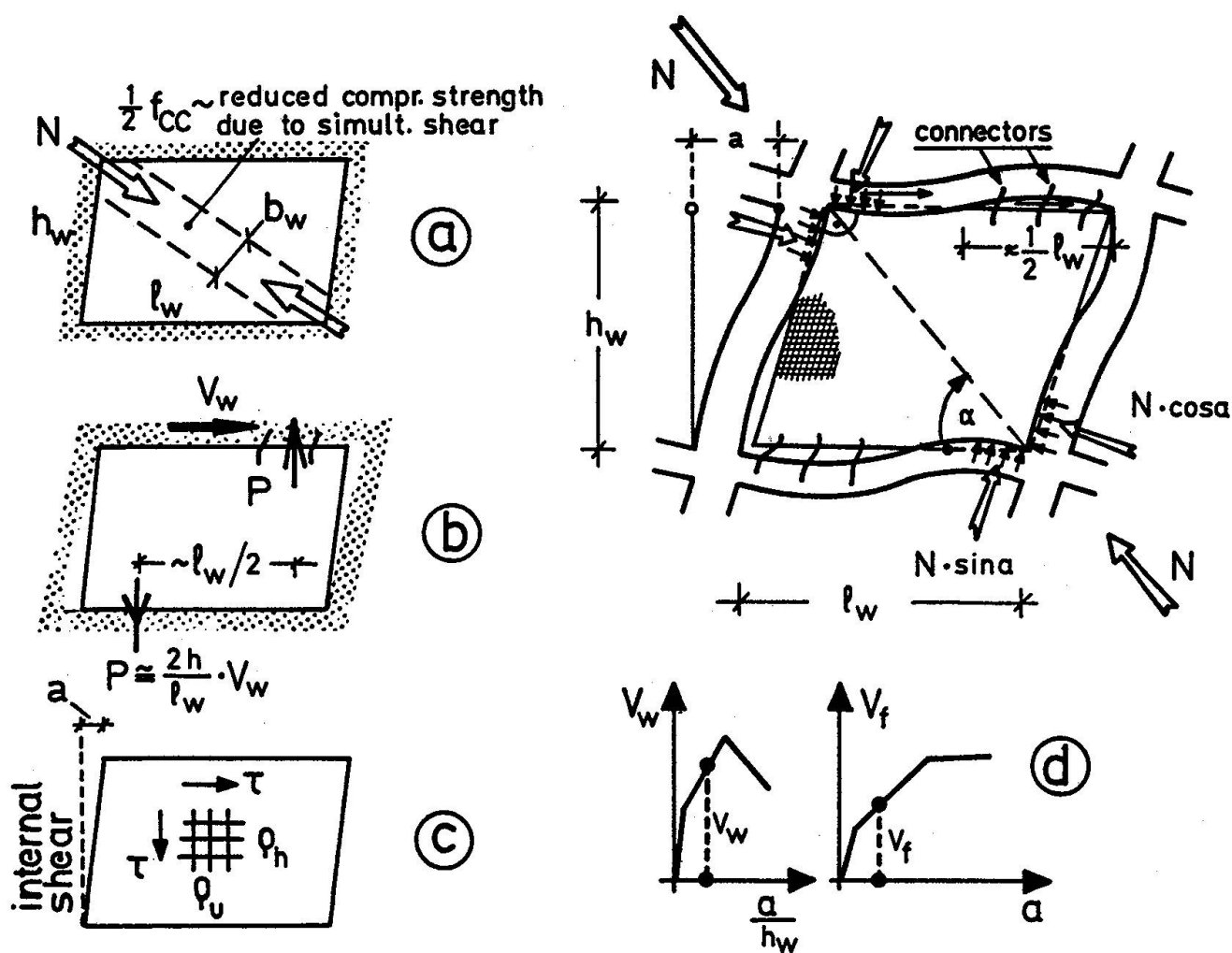


Fig. 44: Oversimplified model for dimensioning of infills



idealised truss model, sub-modeling of constituent linear members (axially tensioned or axially compressed R.C. elements, may be carried-out the same way as in Fig.43, provided that sliding shear is excluded. Step by step increase of horizontal displacement "u" and corresponding analysis of the truss, result in a "v" vs. "u" relationship, including falling branch or even cyclic behaviour (provided appropriate sub-models are available). Therefore, out of a constitutive law of a R.C. wall, a rough assessment of a damaged wall is possible. Input data needed: degree of cracking, possible signs of steel yielding, residual angular deformation, local spalling of concrete, (comp. Fig. 37a).

4.2. Redimensioning

Simple cracking repaired by means of epoxy injections, does not need any re-modeling since such a repair is based on the assumption that the wall is correctly reinforced and detailed.

Jacketing of a damage R.C. wall is meant to: i) bring down the nominal shear stress (stiffer and stronger diagonal compressive strut, comp. § 3.2), ii) provide the necessary additional shear reinforcement.

Two redimensioning problems do arise:

a) Transversal shear connectors should ensure the horizontal load transfer from the damaged wall to the jacket. If the constitutive laws of the two elements are known (s. §II.4.1), the required stress level "τ" should be shared by the existing (τ₀) and the jacket wall (τ_j):

$$\gamma' = \frac{\tau_0}{K'} = \frac{\tau_j}{K_j} = \frac{\tau}{K' + K_j}, \quad (\text{s. Fig. 46}).$$

Therefore, a part $V_j = V \cdot (1 + \frac{K'}{K_j})$ of the total horizontal force "V" will be transferred to the jacket by means of "n" horizontal shear connectors. Each of them has to resist a dowel force

$$D = V \cdot n \left(1 + \frac{K'}{K_j}\right) - \frac{h_w l_w}{n} \cdot \tau_{adh}$$

where "τ_{adh}" denotes a sufficiently low value of the adhesion strength which may be developed at the wall-jacket interface (s. §I.1.2); in principle, such an adhesion is quite reliable in this case of self-cured internal surface.

b) A second problem concerns the dimensioning of the jacket itself (thickness and web reinforcements). To this purpose, the simple friction model used in the Seismic Annex of the CEB-FIP Model Code may be applied here too: (§11.6.5.2.3).

Finally, it has to be noted that the level of future loading of the repaired or strengthened wall is highly affected by the nature of actions expected: Stress-controlled loading equal to that it has damaged the existing wall (s.Fig. 46) leads to higher values of K_j (higher participation $V_j:V$ of the jacket) but lower jacket strength required. On the contrary, strain-controlled actions necessitate lower K_j -values and may need stronger jackets.

Flexural damage of R.C. wall calls for a strengthening of its boundary edge elements, which turns to be essentially a repair or strengthening of columns (§II.2).

4.3. R.C. diaphragms

This is a special case of in-plane loaded building elements. Their possible damages or weaknesses are mainly due to tensional insufficiency; hindered shrinkage and seismically induced tension forces (uneven distribution of horizontal forces to the stiff vertical elements connected to the slab), may produce tension cracks. The necessary additional tension reinforcements are introduced in concentrated zones, mainly along the boundaries of the slab; their resistance is calculated by means of a truss model or a deep-beam model (Fig. 47).

5. MASONRY WALLS

5.1. Residual characteristics

It is much more difficult to assess quantitatively a damaged masonry wall by means of its constitutive law (e.g. under shear loading). Nevertheless empirical diagrammes like that given in Fig. 41 or specifically prepared out of an appropriate model (Fig. 48), may be helpful when an attempt is made to estimate, roughly though, the residual characteristics of a damaged masonry wall.

5.2. Jacketing

Shear connectors may be designed as in the case of R.C. walls' jackets (§4.1.a); appropriate stiffnesses have to be sought in the corresponding constitutive diagrammes (e.g. Fig. 48 for masonry and Fig. 46 for R.C. jacket).

For the total bearing capacity of the repaired (composite) wall, a fully plastic solution (neglecting the incompatibility of deformations) would lead to the following equation:

$$R_{tot} = R_j + \gamma_{n1} \cdot R_{w,res} + \gamma_{n2} (R_{w,0} - R_{w,res})$$

where

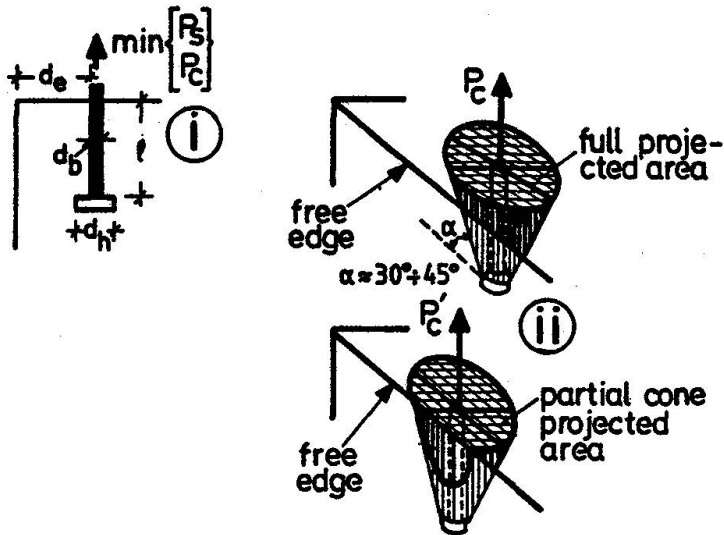


Fig. 45: i) Short anchors with anchorage head
ii) Idealised failure surfaces through concrete

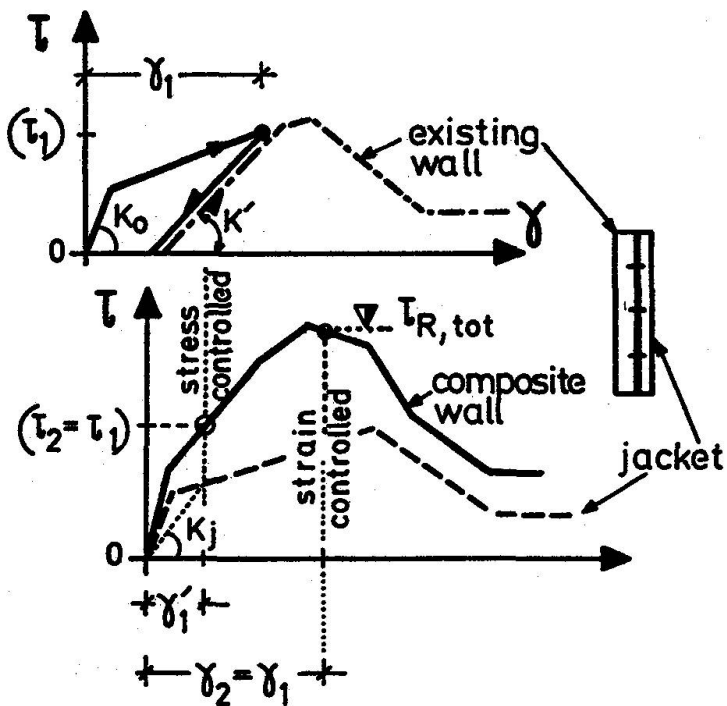


Fig. 46: Combination of existing R.C. wall (damaged at " τ_1 "-shear level and unloaded) with a R.C. jacket; the composite wall is exposed to future stress $\tau_2 = \tau_1$ or to future strain $\gamma_2 = \gamma_1$

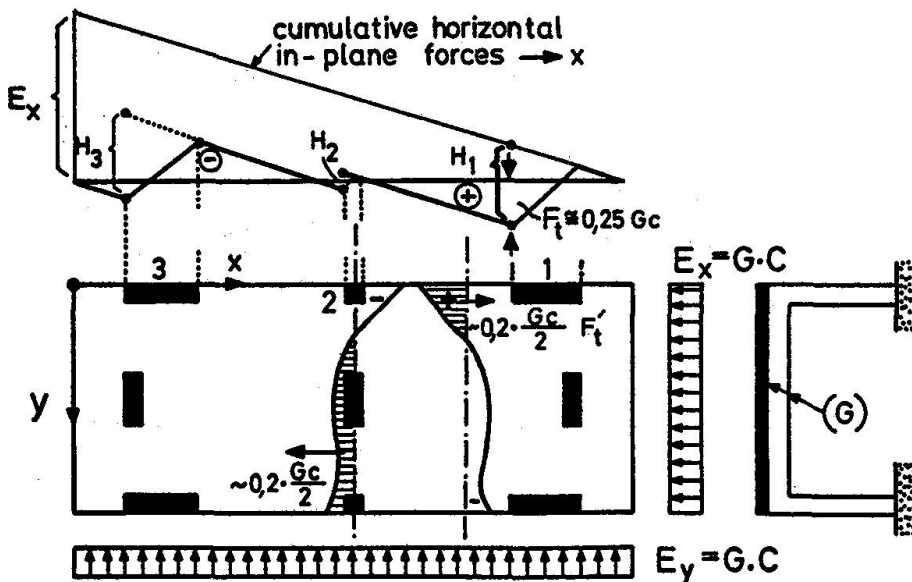


Fig. 47: In-plane tensions in a R.C. diaphragm, due to seismic forces acting at "x" or "y" direction

- R_j = strength of the jacket
 $R_{w,0}$ = initial strength of the masonry-wall
 $R_{w,res}$ = residual strength of masonry-wall
 γ_{n1} = model uncertainty factor related to the incompatibility of deformations

After repair, there is a relatively low probability for full coincidence of the existing cracks and the future cracks of the jacket. Therefore, a certain part γ_{n2} ($\ll 1$) of the neglected difference " $R_{w,0} - R_{w,res}$ " available in the new cracks of the masonry, might be taken into account.

Semi-empirical expressions for estimating the shear capacity of masonry walls:

$$\text{Plain masonry } \tau_{wu} = \frac{2}{3} f_{wt} \sqrt{1 + \frac{\sigma_o}{f_{wt}}}$$

For reinforced masonry, existing experimental data do not allow for a fully quantitative prediction of its strength. Further modeling is needed.

Finally, a simple superposition model has been developed in China (NIU, 1982) for double reinforced mortar jacketing on low quality brick masonries subjected to seismic loading:

$$R_{tot} = \frac{2}{3} \alpha_w R_{w,res} + \alpha_m R_m + \alpha_s R_s$$

where

$$R_{w,res} = \begin{cases} \tau_{wu} \cdot A_w, & \text{non-cracked masonry} \\ 0,7 \cdot \sigma_o \cdot A_w, & \text{cracked masonry} \end{cases}$$

$$R_m = \text{shear strength of the mortar}$$

$$R_s = 2 A_s f_{sy} l_w : \alpha_s$$

$$A_s = \text{cross-section of each bar of the web reinforcement}$$

$$\alpha_s = \text{spacing of bars}$$

(both horizontal and vertical reinforcement is provided)

$$\alpha_w = \begin{cases} 0,10 + 0,06 \cdot \frac{\sigma_o}{f_{wt}}, & \text{non-cracked masonry} \\ 1,00, & \text{cracked masonry} \end{cases}$$

$$\alpha_m = \begin{cases} 1/3, & \text{non-cracked masonry} \\ 0, & \text{cracked masonry} \end{cases}$$

$$\alpha_s = 1,0.$$

For the same repair technique, the stiffness of the composite wall is given by the expression

$$K = \beta \cdot E_w A_w + E_m A_m, \quad \beta = \begin{cases} 1,0, & \text{non-cracked} \\ 1/3, & \text{cracked} \end{cases}$$

where indexes "w" and "m" denote the material of the wall and the mortar respectively.

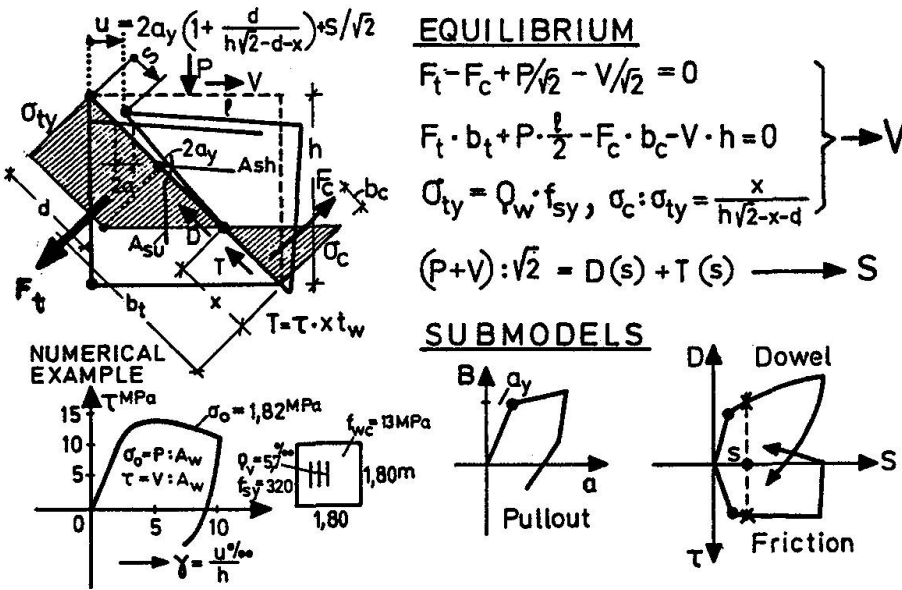


Fig. 48: The stereostatic model for reinforced masonry walls under normal and cyclic horizontal loads

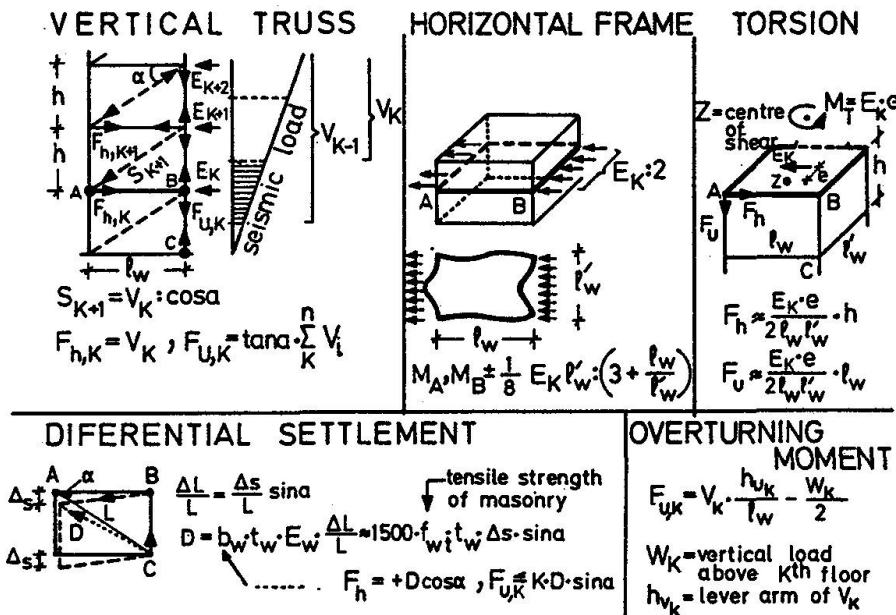


Fig. 49: Oversimplified models for the analysis of strengthening-belts (or horizontal tie-rods) AB and corner - columns (or vertical tie-rods) BC.

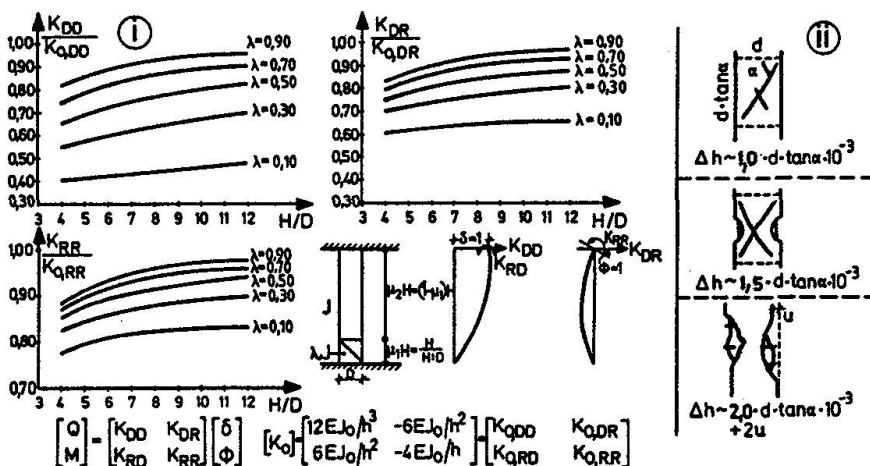


Fig. 50: i) Parametric calculation of stiffness indexes of a damaged R.C. column (Syrmakizis, Voyatzis, 1983)
 ii) Rough estimation of "settlement" of damaged columns

5.3. Reinforcing-belts, corner columns and tie-rods

One of the well known techniques for strengthening masonry buildings (mainly against earthquakes) is to provide additional linear elements along all vertical (internal or external) edges, as well as along all horizontal levels of floors (of both external and internal walls). These linear elements may be R.C. belts and columns or just tie-rods (slightly prestressed, as a rule); all of them should be carefully interconnected.

Simple conceptual models for the spatial analysis of those elements are presented in Fig. 49. More sophisticated models are also available, incorporated in several finite elements programmes for wall systems.

Part III: Re-Modeling of Structures

1. STIFFNESS CONSIDERATIONS FOR DAMAGED AND STRENGTHENED BUILDING ELEMENTS

1.1. **Damaged** building elements are suffering a certain decrease of their stiffness versus deflections (beams and columns), versus axial shortening (columns) and versus angular deformations (walls). As a consequence of such a decrease of stiffnesses, a considerable re-distribution of action-effects is expected: Damaged elements might be alleviated, but intact elements close to the damaged ones are additionally loaded.

Both modifications are important: Lower as it may be an action-effect of a damaged element, it may still be higher than an acceptable percentage of its corresponding residual strength. And, obviously, we wish to know the safety margins left to the adjacent building elements, after their overloading. To this purpose, stiffness modifications after damage should be estimated, even roughly. This is the reason each chapter of Part II of this Report was devoted to a possible estimation of residual characteristics after damage, local stiffnesses included. However, stiffness is a much more difficult characteristic to be modelled than strength.

In any case, as soon as residual stiffnesses $(EJ)'$, $(GA)'$, $(EA)'$ of the damaged length are estimated (possibly as percentages λ_j , λ_G , λ_E of the corresponding initial stiffnesses), the t r a n s f e r m a t r i x method may be used in order to calculate the modified

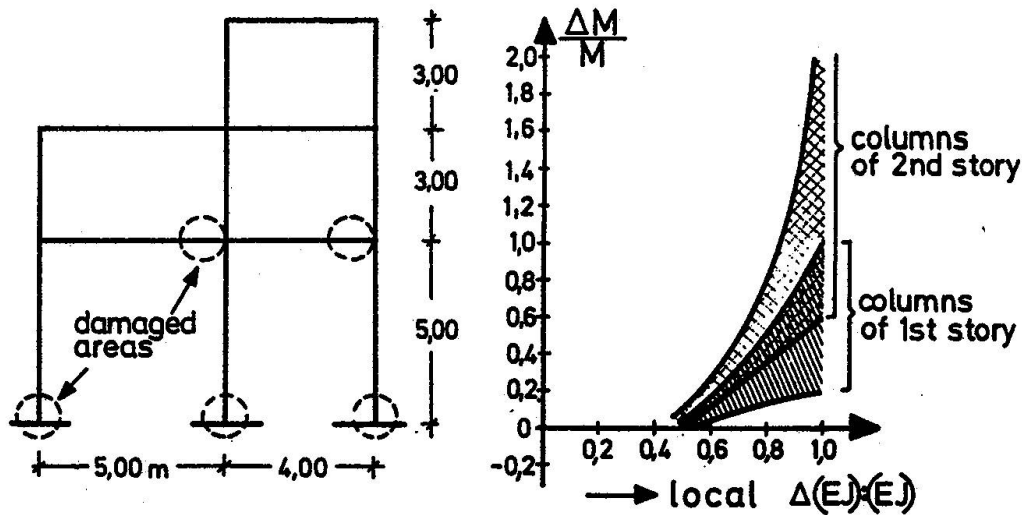


Fig. 51: Only large losses of local bending-stiffness may produce considerable redistribution of action-effects after damage (AVRAMIDOU, 1982)

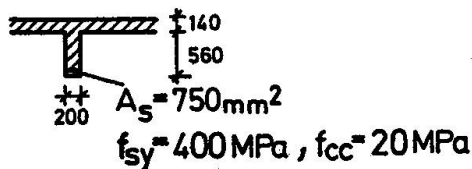
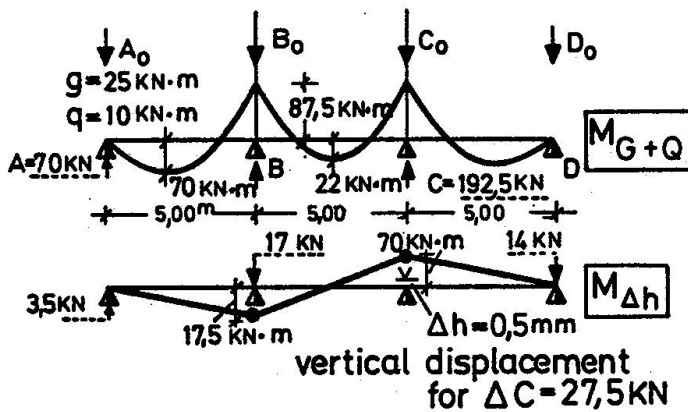


Fig. 52: Redistribution of action-effects due to temporary shoring for repair or strengthening

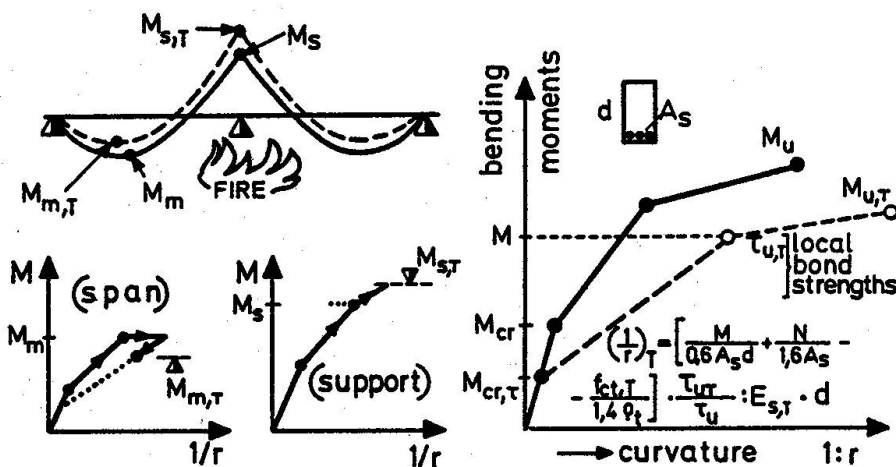


Fig. 53: A two span continuous beam after fire. An oversimplified model for the assessment of the redistribution of bending moments.

stiffness indexes K_{DD} , K_{DR} , K_{RR} , K_L at the end of the building element (D = transverse displacement, R = rotation, L = longitudinal displacement). An output of this technique is given in Fig. 50,i. Redistribution of action-effects is also induced by local settlement of the support of a continuous beam, due to soil conditions or to a local damage of a column; this is a direct cause of redistribution. Imposed delayed deformation due to soil conditions has been repeatedly the subject of modeling, which may also be applied for the case of rapid settlement due to an abrupt damage; however creep effects will not be taken into account in this case. Finally, an estimation of the order of magnitude of this abrupt settlement is attempted in Fig. 50,ii. It is however worth to note that even large percentages of local bending-stiffness losses are not very important for the overall behaviour (Fig. 51).

1.2. **Repaired** building elements are subject to stiffness' increase which is expected to increase the action-effects of these elements when future loads will be applied. Therefore, such stiffness' increase should be somehow estimated, especially in cases of jacketing. To this purpose, a formalistic approach might be first used: Two "envelop" analyses may be carried out on the safe side; one regarding the same element, taking into account the maximum stiffness (initial column plus jacket, as if they were monolithic), and one regarding the adjacent building elements taking into account the minimum stiffness of the repaired element (the mean value of a) the previously used stiffness and b) the sum of stiffnesses of the damaged area and the jacket, as if they were independant). A more sophisticated method could take into account the relative slip between existing column and jacket (comp. §II,2.2).

2. REDISTRIBUTION OF ACTION-EFFECTS

2.1. Due to mechanical actions during the intervention

There is a problem of temporary redistribution of action-effects due to the forces imposed underneath the beams, near the column-beam joints, in order to implement shoring of a damaged column. In ordinary cases, these forces are controlled (as it would be the case if hydraulic jacks were used). However, for such a control it is important to measure also vertical displacements " Δh " imposed during the shoring. Such displacements could be directly in-

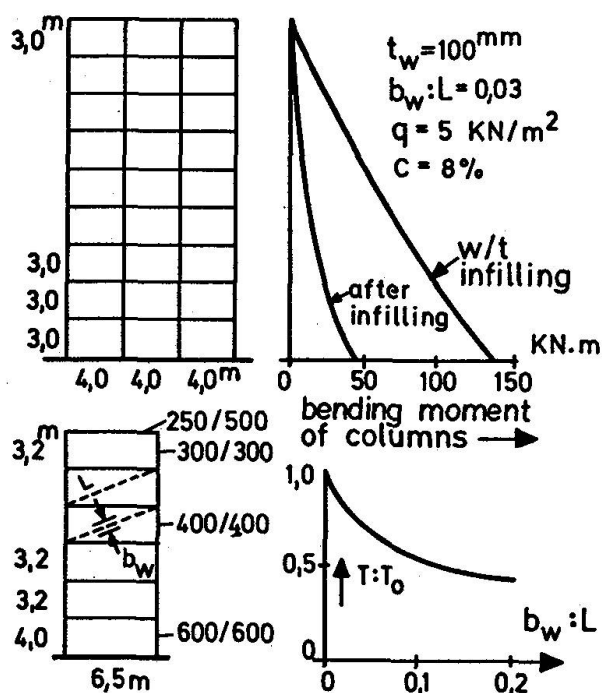


Fig. 54: Infill brick walls, drastically modify the structural behaviour of R.C. frames

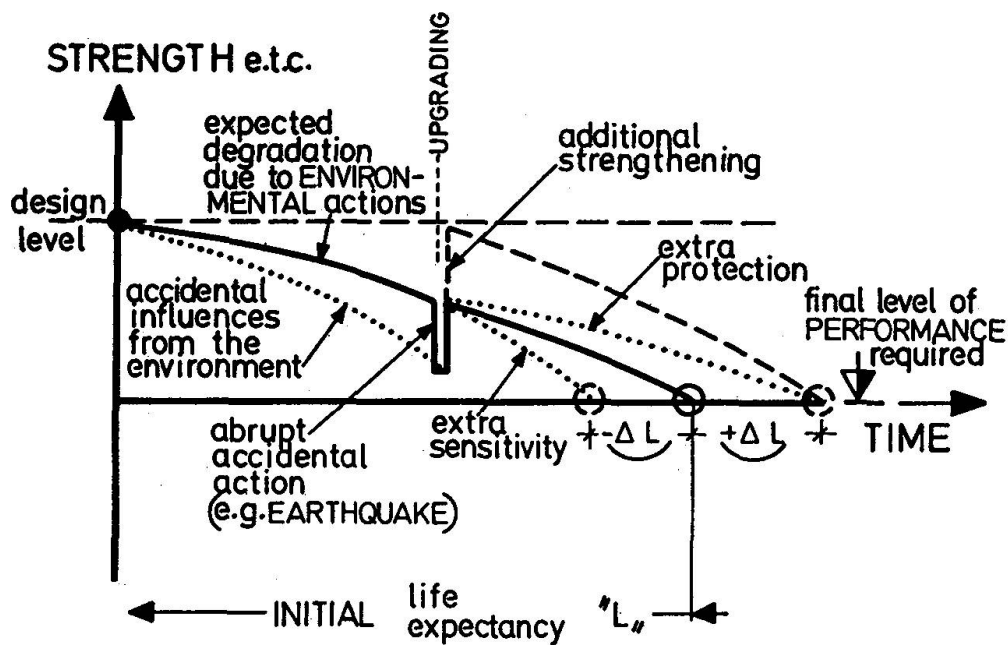


Fig. 55: The degree of upgrading, combined with the intensity of future environmental factors, may adversely influence life expectancy of buildings

roduced into the model of the structure, in order to calculate the corresponding "negative" action-effects induced to the structure after shoring (Fig. 52); **relaxation** should also be taken into account, up to the time of hardening of the concrete additionally used. On the other hand, even rough estimations of the loads undertaken by the temporary supports (a reasonable percentage " λ " of the load "C" previously carried by the column concerned) may lead to some approximate values of redistributed action-effects: If such an unloading equal to $\lambda.C$ is estimated, the column (of composite cross-section "A" and length "h") will be elongated by $\Delta h = \frac{\lambda C}{E'_c \cdot A} \cdot h$, where E'_c denotes a reduced modulus of elasticity $E'_c = E : (1 + \Delta\phi)^C$ to take into account relaxation ($\Delta\phi$ = partial creep factor for the period of repair).

2.2. Due to other actions

After-damage redistribution may be estimated by means of ordinary structural analysis methods, after the assessment of stiffness losses at each point of damage (§1.1). An example, under vertical and seismic loads, is given in Fig. 51.

A particular case of redistribution of action-effects is presented in Fig. 53 concerning a fire-damaged beam. In fact, modeling of stiffnesses' modifications in a hyperstatic system under fire would need a very complicated procedure; therefore more refined models are needed in this field.

After-strengthening redistribution may also be estimated by means of an ordinary structural analysis, provided that the new stiffnesses are known (§1.2). An interesting example is presented in Fig. 54; Multistory R.C. frames have been totally infilled by simple brickwork; bending moments of columns, as well as the fundamental period of vibration of the building were drastically reduced.



Part IV: Reliability Aspects

The typical inequality regarding safety

$$R_d = \gamma_n \cdot r(f_k : \gamma_m) > s(S_k \cdot \gamma_f) = S_d$$

has to be thoroughly reconsidered in the case of repair and/or strengthening.

1) $\gamma_{f,G,exist}$ (for existing dead loads):

Decreased in case geometrical measurements (lengths, heights, sections) and estimation of specific weights have shown that uncertainties of dead loads are lower than those reflected in usual γ -factors. Otherwise, $\gamma_{f,G,exist}$ should be increased.

2) $\gamma_{f,G,add}$ (for additional dead loads):

Decreased, due to lower geometrical uncertainty and better estimation of dead loads ($\gamma_{f,G,add} \approx \gamma_{f,G} - 0.1$). In case of small thicknesses and/or when inspection and control are not satisfactory $\gamma_{f,a,add}$ should be increased.

3) $\gamma_{f,Q}$ (for live loads):

Increased or decreased, depending on:

- life expectancy of repaired/strengthened structure (see Fig. 55).
- nature and frequency of action effect after damage; the "frequency" has to be estimated on the basis of informational data regarding the damaging action-effect).

Generally:

for "frequent" actions: $\gamma_{g,Q}$ should increase

for "accidental" actions: $\gamma_{f,Q}$ should decrease.

For possible unfavourable conditions, in connection with seismic actions, two cases should specifically be mentioned:

- Possible lower natural period of the building

$T'_n = T_n \sqrt{k:k'}$ (where "k" denotes an overall stiffness value) may lead to higher spectral response " β' " and, therefore, to higher base-shear coefficient $c' = c \cdot \beta' : \beta$.

- Possible lower ductilities " μ " after repair (compared to the initial ones " μ ") correspond to a reduction of the behaviour factor K and, therefore, to an increase of base shear coefficient $c' = c \cdot \mu : \mu'$.

When national codes define unique base-shear coefficients for simple structures, the above mentioned eventualities correspond to an increased γ_f value: $\gamma'_f = \gamma_f \cdot \frac{\beta'}{\beta} \cdot \frac{\mu}{\mu'}$

4) $\gamma_{m,exist}$ (for existing materials):Non-damaged elements

Decreased or increased, depending on the results of a large amount of measurements and tests, which may show a decrease or an increase of initially expected uncertainties.

Damaged elements

Damaged areas: "Initial" γ_m -values may be used. However within the new structural models, describing the modified situation, appropriate γ_n -factors are to be incorporated.

Non damaged areas: As in non-damaged elements.

5) $\gamma_{m,add}$ (for additional materials):

- o For additional repair and/or strengthening materials, in recognition of the extra variabilities in construction operations and the limitations of the field control, the following rough $\gamma'_C : \gamma_C$ values could be possibly used for concrete (cast-in-place):

Level of quality control and field inspection	Additional thickness			
	< 100 mm		> 100 mm	
	accessibility		accessibility	
	low	normal	low	normal
High	1.2	1.1	1.0	1.0
Average	1.3	1.2	1.1	1.0

- Whenever welding is carried out, new reinforcements have to be taken into account with $\gamma'_S = 1,2 \gamma_S$, unless full observation of welding specifications is secured.
- When small concrete cracks (≤ 4 mm) have been repaired by means of an appropriate pressure-injected resin, a $\gamma'_C : \gamma_C$ value of about 1.3 should be applied (ATC 3 - 1978).

6) γ_n -factors (correction factors):

Theoretical methods for-dimensioning of repaired sections are not very well developed. Therefore a calibration is needed of the following additional factoring.

Strength:

$$\text{Repair "in line"} \quad R = \gamma_n \cdot \min \begin{cases} R_{add} \\ R_{init} \end{cases}$$

Repair "in parallel" $R = R_{add} + \gamma_{n1} R_{res} + \gamma_{n2} (R_{init} - R_{res})$ where " γ_n " reflect uncertainties of the respons of cross-sections.

Action effects:

There are additional uncertainties due to the redistribution of action effects. Therefore $S_d = \gamma_f (S_{do} + \gamma_{n,s} \cdot \Delta S_d)$

where ΔS_d = additional action-effect due to the redistribution after repair

and $\gamma_{n,s}$ reflects uncertainties of the "believed" redistribution model.



NOTE: Quantitative models for the assessment of partial safety in repaired and strengthened structures may be found in DIAMANTIDES, 1982.

ACKNOWLEDGEMENTS

The collaboration of Mr. M. Chronopoulos is gratefully acknowledged. Material worked-out by the CEB/G.T.G.12 is also included in this Report.

R e f e r e n c e s

1. ARAKAWA T.: "Effect of welded bond plates on aseismic characteristics of R.C. columns", 7 WCEE, Istanbul, 1980.
2. AVRAMIDOU N.: "Redistribution of action effects after damage and repair", CEB/GTG 12 (unpublished report), 1982.
3. BATE, E.H.: "Some experiments with concrete". Reinforced Concrete Review; Vol.4, No. 7, Sept. 1957.
4. BENEDETTI D., CASELLA M.L.: "Shear strength of masonry piles", 7th International Conference on Earthquake Engineering, Istanbul, Sept. 1980.
5. BIRKELAND P.W., BIRKELAND H.W.: "Connections in precast concrete construction", ACI Journal, Mar. 1966.
6. BROMS B.B.: "Design of laterally loaded piles", ASCE, Vol. 91, No SM3, 1965.
7. DASCHNER F.: "Notwendige Schubbewehrung zwischen Betonfertigteilen und Ortbe-ton". Bundesministerium für Raumordnung, Bauwesen und Städtebau Forschungsbericht T 1365, 1976.
8. DIAMANTIDIS D.: "Considerations about safety factors for redesign", Essay supporting the work of CEB/GTG 12, 1982.
9. ELEIOTT A.F.: "An experimental investigation of shear transfer across cracks on reinforced concrete", A thesis presented to the Faculty of the Graduate School of Cornell University for the Degree of M.Sc., June 1974.
10. FARDIS M., BUYUKOZTURK O.: "Shear transfer model for R.C.", ASCE, Journal Eng. Mech. Div., Apr. 1979.
11. FROUSSOS A., TASSIOS T.P.: "Damaged R.C. columns under large plastic deformations", Scientific Papers, Faculty of Civil Engineering, Nat. Tech. University, Athens, 3/1982 (in greek).
12. HANSON N.W.: "Precast-Prestressed Concrete Bridges. 2. Horizontal Shear Connections". Journal PCA, Research and Development Laboratories, V.2, No. 2, May 1960.
13. HETENYI M.: "Beams on elastic foundation", Ann Arbor: The University of Michigan Press, 1946.
14. KLINGNER R., Mendonca J.: "Tensile capacity of short anchor bolts and welded studs: a literature survey, ACI, Journal, July-August 1982.
15. LADNER M., WEBER C.: "Geklebte Bewehrung im Stahlbetonbau", EMPA, Dübendorf, 1981.
16. NIU ZEZHEN: "Earthquake resistant strengthening of brick structures", 7th EAEE, Athens, 1982.
17. SACHANSKI S., BRANKOV G.: "Investigation for determining the size of seismic forces on the evidence of damaged buildings", Proc. of 6th World Conference on Earthquake Engineering, London, Sept. 1972.
18. SHEIKH S.A., UZUMERI S.M.: "Properties of concrete confined by rectangular ties", AICAP-CEB Symposium, Rome, May 1979, CEB Bulletin No.132, Theme 1, Paper No. 7.



19. SHEIKH S.A., UZUMERI S.M.: "Mechanism of confinement in tied columns", Proc. of 7th World Conference on Earthquake Engineering, Istanbul, Sept.8-13, 1980.
20. SMITH B.S., CARTER C.A.: "A method of analysis for infilled frames", Proc. Inst. of Civil Eng., Sept. 1969.
21. STEINWEDE K.: "Statische und dynamische Untersuchungen an nachträglich verstärkten, auf Biegung beanspruchten Stahlbetonplatten", Mitteilungen aus dem Institut für Baustoffkunde und Materialprüfung der Technischen Univ. Hannover: Heft 38, 1977.
22. TASSIOS T.P., TSOUKANTAS S.: "Serviceability and ultimate limit states of large panels' connections under static and dynamic loading", Proc. of the RILEM-CEB-CIB Symposium on Precast Joints, Vol. I, NTU, Athens, 1978.
23. TASSIOS T.P., VINTZÉLEOU E.: "Shear force-displacements characteristics of pre-stressed connections", Idem.
24. TASSIOS T.P., SYRMAKEZIS C., CHRONOPOULOS M.: "Recommendations for Repair", Nat. Tech. University, Athens, 1978, (in greek).
25. TASSIOS T.P.: "Properties of bond between concrete and steel under load cycles idealising seismic actions", CEB Bulletin 131, Apr. 1979.
26. TASSIOS T.P.: "Strengthening methods", Seminar on R+S, Dec. 1980, (in greek).
27. TASSIOS T.P.: "Greek research on R.C. behaviour under fully reversed cyclic actions", (invited lecture), Swedish Cement and Concrete Research, Institute, Stockholm, 1981.
28. TASSIOS T.P., GRISPOS K.: "Response degradation and hysteretic damping of R.C. columns under large cyclic post-yielding deflections", NTU Report, Athens, 1982 (in greek).
29. TASSIOS T.P.: "The mechanics of column repair with a R.C. jacket", 7th ECEE Athens, 1982.
30. TASSIOS T.P., PAPARIZOS L.: "A simple model for pull-out/push-in cyclic actions", (unpublished), 1982.
31. TERCELY S., SHEPPARD P.: "The load carrying capacity and deformability of reinforced masonry walls", 7th International Conference on Earthquake Engineering, Istanbul, Sept. 1980.
32. VALLENAS J.M., BERTERO V.V. and POPOV E.P.: "Hysteretic behaviour of Reinforced Concrete structural walls", UCB/EERC, 1979.
33. VASSILIOU G.: "Behaviour of repaired R.C. elements", Ph.D. Thesis, NTU of Athens, 1975 (in greek).
34. VERDEYEN J., GILLET J.: "La résistance transversale des fondations sous l'effet de charges horizontales", Université Libre de Bruxelles, Apr. 1967.
35. VINTZÉLEOU E., TASSIOS T.: "Dowel action under cyclic loading", 7th Symposium on Earthquake Engineering, Roorkee, 1982.
36. WALRAVEN I.: "Mechanisms of shear transfer in cracks in concrete: A survey of literature, DELFT, University of technology, Report 5-78-12, Dec. 1978.
37. YAMADA M., KAWAMURA H., KATAGIHARA K.: "R.C. shear walls without openings", ACI SP42, 1974.
38. KRIPANARAYANAN K.: Discussion on article "Guide to the design of anchor bolts and other steel embedments" by Cannon R., et al., Concrete International, July 1982.
39. ELINGENHOUSEN R. et al: "Local bond stress-slip relationships of deformed bars under generalized excitations", 7th ECEE, Athens, 1982.
40. TASSIOS T., SKARPAS A.: "Shear transfer through cracked R.C. sections" (unpublished), 1982.

Leere Seite
Blank page
Page vide